Quantic Behavior of Turbulence

C.Çıray*, I. Kabakci, E. Bekoğlu***, I. Çolak*****

*C.Çıray, Ph.D; DIC; MS. Prof. (Em.) of Fluid Mechanics. Aerospace Eng. Dept. METU.
e.mail: cciray@metu.edu.tr

**İ. Kabakci, MS. in AS Eng. Roketsan – Ankara.

***E. Bekoğlu, MS. in AS Eng. Ph.D candidate at Imperial College London.

****I. Çolak, MS in AS Eng. Ph.D candidate at AS Department, METU, Ankara.

We seem to be left at present with the loose idea that whenever oscillations in space are coupled with oscillations in time through a dispersive relation, we expect the typical effects of dispersive waves.
G.B. Whitham
(Linear and Nonlinear Waves, p:369)

Abstract

This paper considers a turbulence paradigm which helps to analyze some features of turbulence structure at a physically acceptable level. Highlighted features are dispersion relation, length, and time scales for the whole wave number range of turbulence including one-dimensional energy spectrum. The lowest wave number is restricted only by the dimensions of the domain in which turbulence is active. The highest wave number is limited by measurement capabilities. The physical paradigm conceived for turbulence suggests a combined "particle + dispersive-wave" character of turbulence", shortly "Quantic Behavior of Turbulence (QBT)". QBT studies turbulence starting from the molecular activity of fluid particles in a turbulent flow. Coagulations of molecules are demonstrated via numerical simulation of molecular activity for different mean velocities. These groupings of fluid particles can be considered as "infant eddies". A possible physics for the formation of eddies that characterizes the "discrete nature" of turbulence at low frequencies and associated "dispersive-wave behavior" at high frequencies, is explained. This reasoning leading to define fluctuating velocity as group velocity is discussed."Calculation of Wave Number" in view of QBT is performed with the help of two equations and an auxiliary relation. The first equation is a physical relation that uses the energy spectrum and the other one is the group-velocity formulation. Related mathematical developments are given in the "Appendix". Results from different types of flows are illustrated. Salient features of numerical results are exposed. The dispersion relations of different flows are presented. The discrete + wave-like nature of turbulence is highlighted in view of an overall evaluation in "Discussion" at the end of the paper.

Introduction

The assertion that "Turbulence is a "continuum" phenomenon is generally accepted [Lelele S. K, 1994]. The word "phenomenon" of the assertion seems to be used in the sense of the "physical nature" of turbulence. It may also refer to "mathematical ease" provided by "continuous mathematics" to handle turbulence. Continuum consideration is handy from mathematical point of view. Yet, from physical point of view, the existence of eddies indicates "discrete character" to be a strong characteristic of the "nature" of turbulence. Indeed, the population of eddies is responsible for almost all kinetic energy and functions of turbulence.

It is reasonable to consider an eddy as a grouping of fluid particles (molecules) which have chosen to move together for a while. The properties of an eddy can be accounted for as follows:
1: Eddy formation is a random process. The translational movement of molecules in a common direction is the primary factor for the formation of coherent structures or eddies.
2: The lifespan of an eddy is limited. The group or eddy forms and at the end of its lifespan it disperses.
3: The size, shape, mass, and energy content of an eddy define its "identity" during its lifespan.
4: During their existence, eddies perform random motion known as the "fluctuating" velocity of turbulent flow.
5: Identity elements are randomly shared between eddies.
6: The word "Particles" in the definition of "eddy" is a generic name for "molecules" and "sub-groups of particles" that form the eddy.
7: An eddy is a package of energy and exhibits a dispersive wave or a dispersive wave-like character.

Discrete and wave-like features have been combined as "Quantic Behavior of Turbulence" or QBT. *But this paper does not say that "turbulence is a Quantum Phenomenon"*. Since the introduction of the turbulence notion in the historical Reynolds' paper [Reynolds O, 1883], the use of continuum formulations led to consider turbulence as a continuum phenomenon. Calculations based on the continuum approach have been, no doubt, satisfactory and useful for many needs of engineering.

On the other hand, the perception of turbulence as a discrete phenomenon is used at the onset independently and successfully by Taylor [Taylor G. I., 1915] and by Prandtl [Prandtl L. Z, 1925] in their "mixing length" theory of turbulence, though they did not use the word "discrete". Their common approach was their conviction for the existence of lumps of fluid particles, each conserving its 'identity' for a while. The conserved quantity was momentum in the case of L. Prandtl and vorticity in the case of G. I. Taylor (ref. cited).
The other feature i.e.: wave-like behavior of turbulence is used to advantage through Fourier or Wavelet transformations for the description of turbulence structure [Kai Schneider and Oleg V. Vasilyev, 2010].

A Paradigm Of Turbulence

General: From the physical point of view, turbulence is essentially an assembly of randomly moving and randomly created eddies.

The word **turbulence** refers only to fluctuating part(s) of quantities (pressure, velocity…) of turbulent flow since in the present exposition this part of turbulent flow will be under consideration. Yet, it is clear that turbulence as such cannot exist and persist without so-called mean flow. Mean flow or main flow velocity plays a central role, either at turbulence scale (in the sense used here) or at RANS or FANS equations level.

One-dimensional (1D) treatment of turbulence kinematics of incompressible fluids is the material of this paper. Yet, there is no restriction to apply the physical perception and related mathematics to 2D or 3D turbulence.

Some characteristics of fluctuating velocity components may be repeated: Firstly, they are **integral parts** of the instantaneous velocity. Secondly, they are **random functions** of space and time. Thirdly, in general, their magnitudes are smaller than that of mean velocity by a factor less than 0.3.

At the end of calculations results of QBT that will be presented in the sequel, any result pertaining to a frequency smaller than 1 c/s is rejected since $f < 1$ c/s is considered as a consequence of the unsteadiness of turbulent flow from the physical point of view. So, 1 c/s is used as a reference for minimum frequency just for the sake of comparison. Yet, $f < 1$ c/s and associated other quantities (wave numbers scale...) can be calculated in terms of QBT.

Particle and Eddy: The word "particle" is a generic name to specify the fluid substance of an eddy, basically "molecules". However, some groups of molecules may also be taken as particles. The term "eddy" defines any coherent agglomeration of particles which have chosen to move together for a certain while. Coherence is understood as the existence of a meaningful correlation of particles forming the eddy.

The motion of an eddy is random. Its size cannot exceed the dimensions of the domain in which turbulence is generated [Landau-Lifshitz, 1959. pp: 118, first three lines]. The physics behind this argument is that boundaries of flow domain limit also fluctuating velocities associated with the coherent structure, either when the motion ceases because of a solid boundary or when a uniform flow (or no flow) becomes the boundary. Therefore, the size of a coherent structure cannot protrude from these boundaries. Hinze considers the smallest sizes of eddies to be not smaller than the conventional "micro-scale" of turbulence [Hinze J. O. 1959, page: 276]. Yet, any explanation for stopping the smallest size of eddies at the micro-scale is not noticed.

While eddies are moving under the effect of a mean flow, the velocity of an eddy is composed of local mean velocity plus its own particular random motion, namely "fluctuating velocity". The fluctuation velocity of an eddy is necessarily an association of velocities of particles that form the eddy.

The definition of "eddy" implies that the life of an eddy has a limited duration. At the end of its lifespan, the coherence of particles forming the eddy is lost, and the eddy is dispersed. This fact will lead to the dispersive nature of wave-like behavior associated with the motion of eddies. During their lifespan, eddies have their own geometric, kinematic, and dynamic properties. The statistical evaluation of these properties leads to understand the 'structure of turbulence'.

How eddies are formed: One can begin by observing the motion of molecules. Molecules of static fluids move randomly in three dimensions, at velocities of about a few hundred m/s for gases as observed in the simulations of Argon at 300K which gave the RMS of molecule speeds as 432.9 m/s [Eneren P., 2016], and with a more refined calculation 432.8 m/s [Kabakci I., 2019]. The motion of any particle is influenced when molecules are subjected to move in a common direction with a certain velocity. This velocity can be named "bulk velocity" and it corresponds to the familiar "temporal-mean velocity". The continuous directional constraint imposed by bulk-velocity forces molecules to move closer to each other while they are also forced to reduce their individual random motion (and

velocities) as a consequence of closer distance between them. As a result, they form groups of molecules which grow till the aggregate is in conformity with the definition of an eddy.
The formation of "infant aggregates" by molecules has been observed in the molecular simulation of Argon at 300K when the quasi-static molecular activity is subjected to a bulk velocity, **Figures 1** and **2**. Figures are selected from a set of five Test Cases [Kabakci I., 2019]. The figures below are related to TEST Cases I and II.

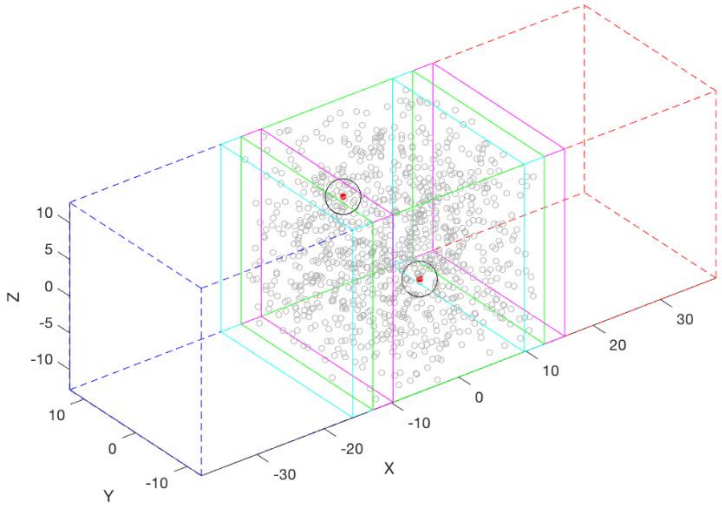

Figure 1: **Particle Formation. TEST I. Argon at 300K, U_{bulk}= 89 m/s. 2 particles and each with 14 molecules [Kabakci I., 2019].**

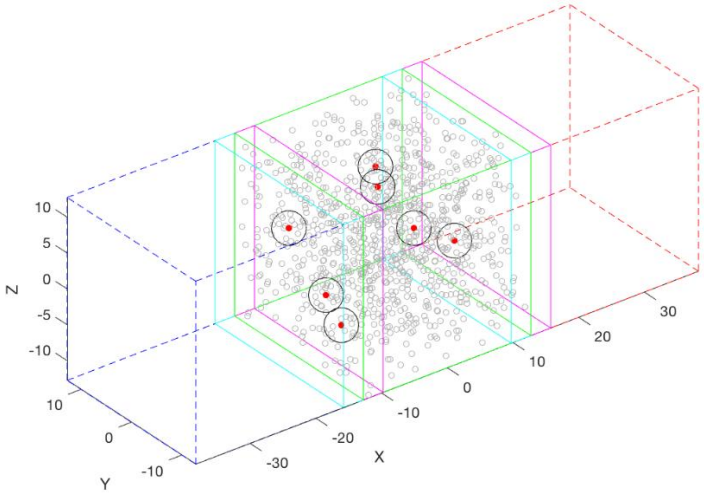

Figure 2: **Particle Formation. TEST II. Argon at 300K, U_{bulk} = 223m/s. 7 Particles and each with 13 molecules [Kabakcı I., 2019].**

TABLE 1: Bulk velocity, the number of aggregate and molecules in aggregates of TEST CASES.

TEST	U_{bulk}	Aggregate	Molecules in Aggregates
-	m/s	-	-
I	89	2	14
II	223	7	13
III	447	1	16
IV	894	4	18
V	2233	1	24

Though the analysis of data generated during the simulation of infant eddies is not complete, the first results indicate that the number of molecules forming infant aggregates increases with increasing bulk velocity, **TABLE 1**.

Since an eddy is a collection of particles having a common motion in the statistical sense, this is coherence. It entails the discrete character of turbulence and the identity of the eddy, **Figure 3**. Yet, eddies do not persist to maintain the coherence indefinitely and they disperse to end their lifespan.

Wave-like Behavior and Group Velocity: The kinetics of an eddy is **reflected (or perceived)** as a wave[1] which is the combined effect of activities (kinetic energies) of particles forming the eddy. When the togetherness of particles ceases, the wave behavior of the eddy is lost.

Since an eddy is composed of particles, its kinetic energy can be depicted as the kinetic energy of a wave packet during its lifespan. Indeed, the kinetic energy of particles forming the coherent structure behaves like "pilot waves" with close wave numbers and gives rise to a wave package appearance, **Figure 3**. Therefore, the velocity of translation of the kinetic energy of this eddy is the "group velocity" which is at the same time the translational velocity of the eddy. The unicity of group velocity with energy transport velocity and translation velocity is shown to be true by Lamb [Lamb, 1962], de Broglie [a reference of Incropera, 1974], and Whitham [Whitham, 1974].

In sum, during the lifespan of the eddy, it has a **discrete** nature. During this period, the identity is conserved at an acceptable level. On the other end, the perception of eddy activity is reflected as a **dispersive wave.** This combined behavior is labeled "Quantic Behavior of Turbulence", QBT for short.

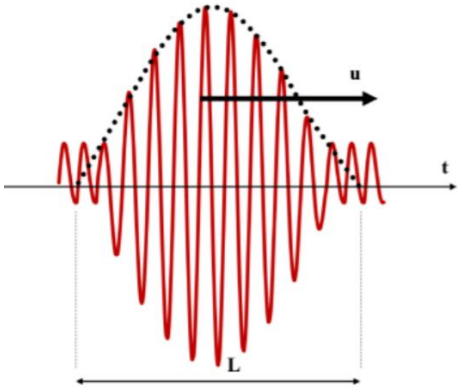

Figure 3: Conceptual Figure of Particle and Wave-like Behavior of an Eddy.

Wave number: A consequence of QBT is that fluctuating velocity "*u*" of turbulent flow is a "group velocity", [Çıray C., 1980, 2017]. Therefore:

$$u = \frac{d\omega}{dk}, \tag{1}$$

where "ω" and "k" are respectively circular frequency and wave number of turbulence. The relation (1) can be considered as an alternative to the well-known expression:

$$k = \frac{\omega}{\overline{U}}, \tag{2}$$

where $\overline{U}$ is the time-averaged instantaneous velocity of turbulent flow and the relation is a consequence of the "frozen turbulence" concept, [G.I. Taylor,1938].

The literature contains a respectable number of papers that use the relation (2). Most of these papers exist in [de Kat R. and Ganapathisubramani B., 2015] and [Bekoğlu E., 2021]. Few of them discuss the validity of the frozen turbulence hypothesis which is the basis of (2). On the other hand, the common approach to calculate wave numbers consists of trying to find ways to remedy the relation (2) which is in fault to predict wave numbers at low frequencies. In essence, they maintain the relation (2) and try to find a suitable "convection velocity, U_C" to replace "$\overline{U}$" in order to satisfy physical properties associated with wave lengths of turbulence. One of these properties is that the largest eddy size can at the most be of intrinsic dimensions of the domain in which turbulent flow takes place [Landau - Lifshitz, 1959. pp: 118, first three lines]. Therefore, it may be inferred that the minimum frequency corresponds to the relevant largest dimension of the turbulent flow domain. Then, it is possible to calculate the

[1] "..a wave is any recognizable signal that is transferred from one part of the medium to another with a recognizable velocity of propagation." (From Linear and Nonlinear Waves. G. B. Whitham (1974). pp: 2, line 10 from the bottom of the page).

minimum frequency from (2). One finds this frequency to be around 200 c/s. This leads to a lack of consideration of turbulence energy in the frequency range of 0-200 c/s which is not negligible.
This paper suggests calculating wave length using (1) which is the consequence of QBT.

Calculation Of Wave Number

Wave number as the consequence of Group velocity: One of the results from the turbulence paradigm described in the previous section is:
"*The fluctuating velocity is the group velocity of the wavy pattern signaled by the eddy, i.e.:*

(1) $$u = \frac{df}{dk}.$$"[2]

The definition of wave number in terms of group velocity, i.e. (1), is not sufficient to calculate wave number (k), as a function of frequency (f) or the "dispersion relation":

(3) $$k = f(f).$$

Therefore, a complementary relation is needed.

Complementary Equation: A relation between "u" and "f" is sufficient to close the gap, i.e.:

(4) $$u = u(f).$$

Then, the solution of:

(1) $$u(f) = \frac{df}{dk}$$

will provide (3). Therefore, the triple connection between "u", "f" and "k" can be realized.

Complementary Equation and Use of a Probability Density Function: Eddies are elements which transport and transfer the kinetic energy of turbulence. The energy spectrum of turbulence shows the partition of this energy between eddies in terms of frequency (and wave number). Therefore, it appears logical to use the energy spectrum *G(f)* within the complementary equation. In addition, a spectrum is specific to a turbulent flow and may help to find (3) pertinent to the flow in question. Then, it is possible to obtain (4) using a pre-accepted probability density function (PDF) of normalized fluctuating velocity "x" through the "complementary equation (6). The complementary equation is based on equality:

(5) $$\int_{-\infty}^{\infty} P(x)u^2 dx = u' \int_0^{\infty} G(f)df \ ,$$

where *G(f)* is twice the normalized kinetic energy per unit mass and frequency. Therefore, its integral shown on RHS of (5) is unity. Physically, the relation (5) means that the kinetic energy of turbulence calculated in the frequency domain is the same when it is calculated with the help of a proper PDF of velocity fluctuations, *P(x).*
For convenience, the following relations are used for non-dimensionalization:

$$U = \overline{U} + u = \overline{U}\left(1 + \frac{u}{\overline{U}}\right) = \overline{U}\left(1 + \frac{u'}{\overline{U}}\frac{u}{u'}\right) = \overline{U}(1 + Ix) = y\overline{U} \ ,$$

where

$$x = \frac{u}{u'} \ , \ I = \frac{u'}{\overline{U}}, \ y = \frac{U}{\overline{U}} = 1 + Ix$$

and "U" is the instantaneous velocity, and "u'" is the root-mean-square of velocity fluctuations.

It is proposed to apply (5) in intervals "$-u$" to "$-u-\Delta u$" and "u" to "$u+\Delta u$". Then, we obtain the complementary equation (6):

(6) $$\int_{-x_i}^{-x_{i+1}} P_L(\xi)\xi^2 d\xi + \int_{x_i}^{x_{i+1}} P_R(\xi)\xi^2 d\xi = u' \int_{f_i}^{f_{i+1}} G(\eta)d\eta \ .$$

[2] Frequency "f" in c/s is used in the sequel.

Equation (6) states that kinetic energy in the ranges "$-u_i$" to "$-u_i - \Delta u$" and "u_i" to "$u_i + \Delta u$" occur at the same frequency band "f_i" to "f_{i+1}" but **may** have different probabilities, **Figure 4.** Indeed, P_L and P_R represent the left and right branches of the PDF if it is chosen to be skewed. The PDF used in the application [Çıray C., 1980], is an extended form of Maxwell-Boltzmann distribution. It is:

(7) $$P(x) = P(1)\, y^n \exp\left\{A^n \left(1 - y^n\right)\right\}$$

with $y = 1 + Ix$ and:

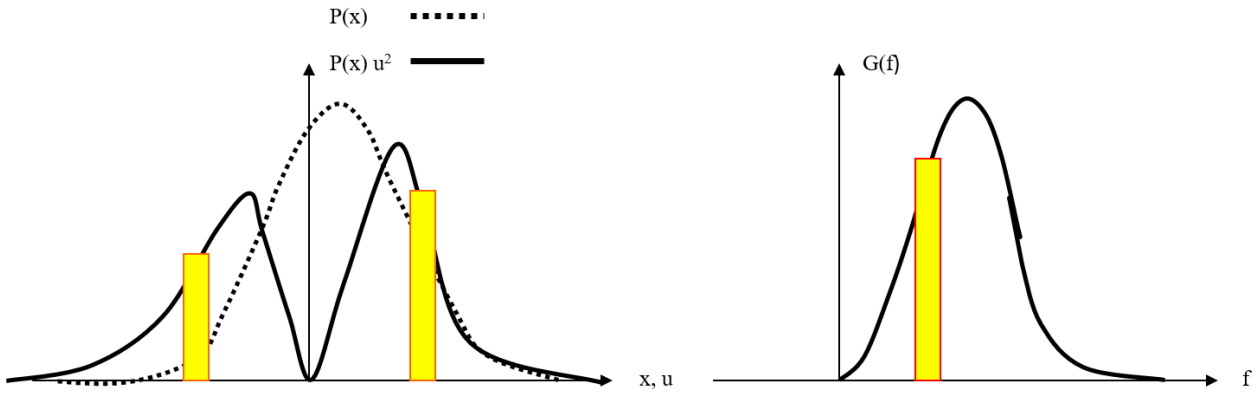

Figure 4: Schematic of Equation (6).

(8) $$A = \frac{\Gamma\left(\frac{n+2}{n}\right)}{\Gamma\left(\frac{n+1}{n}\right)} \quad \text{and} \quad P(1) = I \frac{nA^{n+1}}{\Gamma\left(\frac{n+1}{n}\right)} \exp\left\{-A^n\right\}.$$

$\Gamma(z)$ is the Gamma function of the argument "z" expressed as required in terms of "n" which appears in PDF. The choice of this PDF is reminded of the Maxwell-Boltzmann distribution of speeds of simple molecules. The PDF in question (7), leads to think that the random motion of eddies has a certain resemblance to molecular activity. The constants "A" and "$P(1)$" are obtained from conditions that a PDF has to satisfy. These are: the zeroth moment must be unity and the first moment must be the expectation or the mean velocity, i.e.: The second moment "μ^2" is calculated with the help of (9) which is at the same time equal to "$1 + I^2$",

(9) $$\mu^2 = \frac{\Gamma\left(\frac{n+1}{n}\right)\Gamma\left(\frac{n+3}{n}\right)}{\left[\Gamma\left(\frac{n+2}{n}\right)\right]^2} = 1 + I^2.$$

It is preferred to present mathematical developments as an Appendix at the end of this paper. The "κ^{th}" moment, "μ^{κ}", is given as the formula (25) in the Appendix.

PDF (7) and the Histogram of "*u*": As can be seen in **Figure 5**, non-dimensional histograms $H(x)$ of turbulence and the corresponding PDF given in (7), show remarkable numerical (therefore, geometrical) resemblance [Bekoğlu E., 2021] and later [Çolak I., 2022]. These references contain numerous Figures of the type shown in **Figure 5** for turbulent boundary layers on flat plates, earth-boundary layer (obtained in a wind tunnel), axisymmetric turbulent jet, and turbulent boundary layers with active grids.

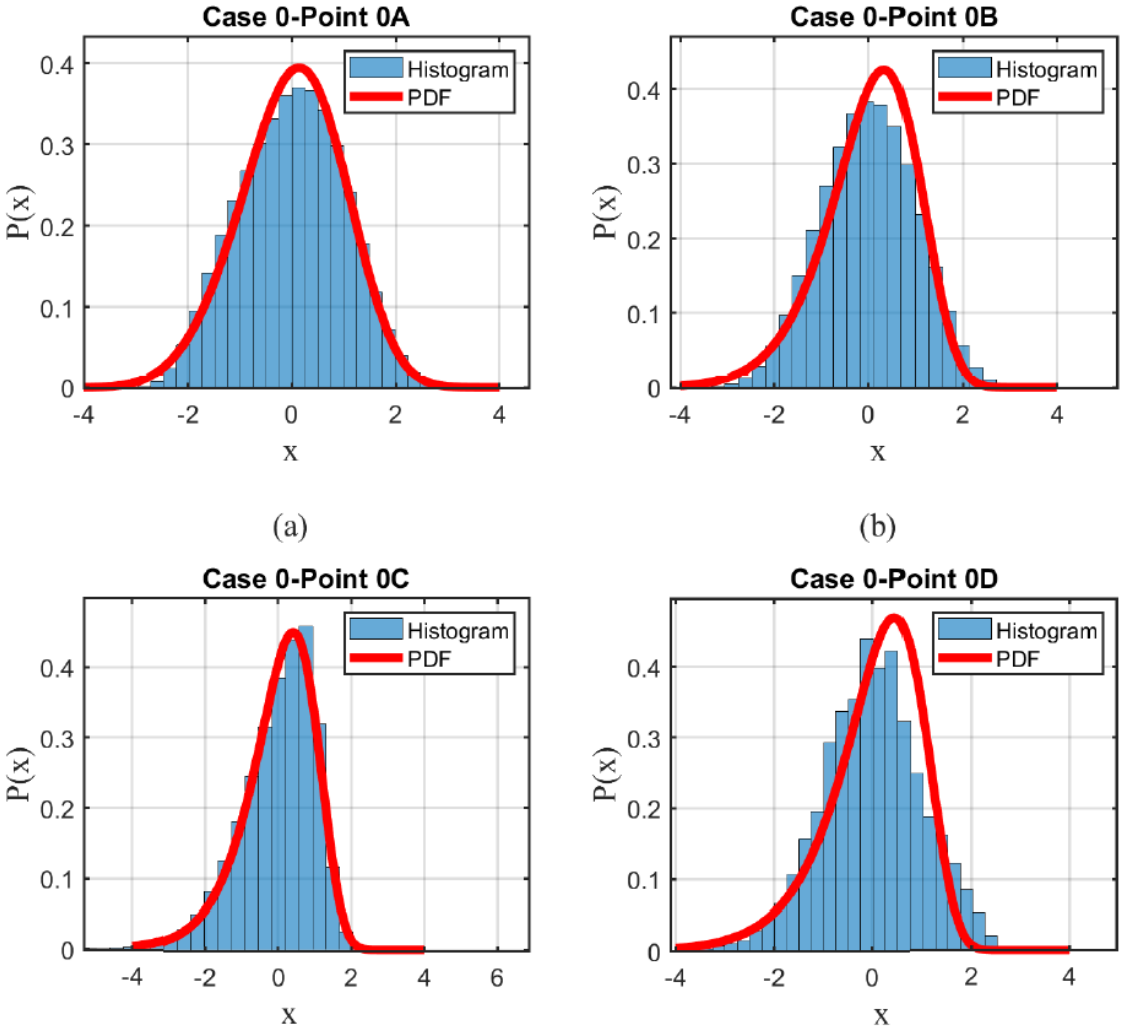

Figure 5: PDF (7) and Histograms for TEST CASE 0.

The Figure is obtained by [Bekoğlu E., 2021] from instantaneous velocity-time-series measured in a canonical Turbulent Boundary layer [Doğan E. et al., 2016].

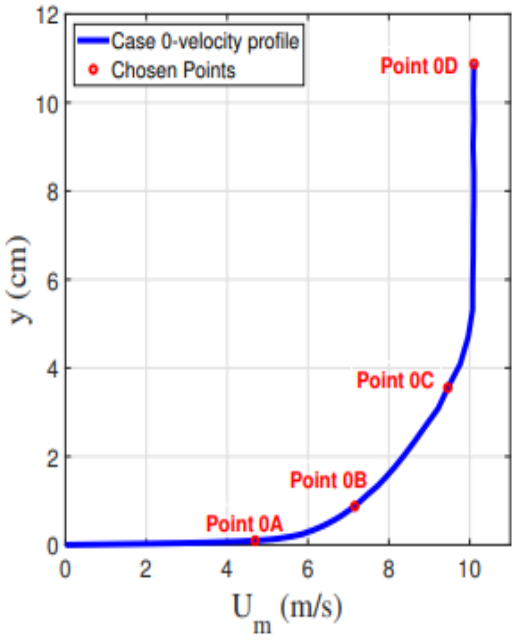

Figure5A: Complementary information for Figure 5 [Bekoğlu E., 2021].

TABLE 2: Complementary information to Figure 5 [Bekoğlu E., 2021].

Point	y [cm]	U_m [m/s]	u' [cm/s]	I_{act} [%]	I_{calc} [%]	n [-]
Point 0A	0.10	4.67	103	21.9	21.9	4.63
Point 0B	0.87	7.16	73.7	10.3	10.3	11.1
Point 0C	3.55	9.46	42.4	4.48	4.48	27.2
Point 0D	10.9	10.1	7.11	0.70	0.70	181

Short Note On Calculation Procedure

Turbulence intensity, I_{act}, is supplied as one of the parameters (for example from experiments) at the point of interest. Therefore, μ^2_{act} can be calculated. Using (8), the corresponding "n" can be found. Within the context of this work, a list of μ^2_{calc} is prepared for a number of "*n*" values. Then, "*n*" corresponding to the problem in hand is determined by matching μ^2_{act} with μ^2_{calc} .

Solution of the algebraic form of (6) for successive intervals, yields a numerical relation between "*u*" (or "*x*") and "*f*" i.e.: (4). Such numerical relation can be seen between columns 1 and 3 of **TABLES 3** and **4**. Then, the solution of (1) determines "*f*" as a function of wave number "*k*", i.e.: the dispersion relation (3). The calculation procedure may be changed by replacing PDF (7) with the histogram which is likely to produce results closer to the natural event.

Some Results

Relation Between Eddy Properties (u, f, k, G, P_L, P_R)

Applications of QBT to some turbulent flows are presented in three groups. The first group is based on two test cases (out of ten) drawn from the first paper on the subject [Çıray C., 1980]. The second group contains a set of results calculated for turbulent boundary layers under different conditions [Bekoğlu E., 2021]. Similar treatment of QBT for a turbulent jet will be the last group [Çolak I., 2022].

Frequencies 10^0c/s, 10^1c/s, 10^2c/s, 10^3c/s, and 10^4c/s are selected to compare scales, PDFs… etc. of different flows. Though 1.0c/s appears as the minimum frequency of the turbulence, with the premise that "minimum frequency occurs at the intrinsic dimension of the domain", a minimum frequency can also be defined and calculated.
PDF and histogram graphics are illustrated in Second and Third Groups results. Spectra in terms of wave number are shown in graphical form for all cases.

Numerical results of the triple connection between "*u*", "*f*" and "*k*" are given only for "First Group" just to maintain the paper at a reasonable size. Yet, results presented in **TABLES 3** and **4** have similar trends for the Second and Third Groups.

First Group Results

Numerical results of TEST CASE §2 are shown in **TABLE 3** and those of TEST CASE §8 in **TABLE 4.** They are chosen from a set of ten Test Cases [Çıray C., 1980]. Associated energy spectra in terms of wave number are given in **Figures 6** and **7.** Relevant information for each flow is supplied at the heading of tables and figures.

The data for TEST CASE §2 belongs to hot-wire measurements performed at 4.00 cm downstream of the leading edge of a NACA 0012 airfoil of 30 cm chord and 30 cm span with tip-plates. The measurement point was at a distance of 0.67 cm from the upper surface. Therefore, the hot-wire was approximately 10.00 cm from the ceiling of the wind tunnel, since the mid-point of the airfoil was 15.00 cm from the ceiling of the wind tunnel and at an angle of attack of 12^o.

TABLE 3 (as well as **4**) of TEST CASE §2 is self-explanatory. The wave number and the wave length are shown in columns 4 and 5 respectively. PDF values of "+" and "-" non-dimensional fluctuating velocities i.e. "*x*", appear in the last two columns of **TABLE 3**.

The wave length "*L*" for frequency 1.0 c/s in TEST CASE §2 is 7.645 cm. It is reasonably smaller than the gap between the airfoil and the ceiling of the wind tunnel. Magnitudes of turbulence velocities increase with frequency up to five times of "*x*" at minimum frequency.

Positive fluctuations (+*x*) have a larger probability than negative ones that can be observed in 6 and 7. columns of **TABLES 2** and **4**. The creation of an eddy is an event of a certain probability. Hence, both positive and negative fluctuations must have the same probability for a given eddy.

It can be seen from the P_L and P_R columns that "+*x*" is associated with "-*x*" of smaller magnitude and frequency (or vice versa) for the same probability. This phenomenon is judged as the mechanism leading to rotational movement

and two spear-like (or crescent-like) appearance of the structure. Similar observations can also be made with measurements of Rotta related to the transition region in a pipe (commonly referred as "intermittency"), **Figure 7** [Schlicting H., 1960].

TABLE 3: Data and Characteristics of TEST CASE §2.

$\overline{U}$ = 32.22 m/s I_{actual} = 0.0354 n = 35 A = 0. 98355565

u' = 135 cm/s $I_{n=35}$ = 0.0352 $P(1)$ = 0.4088

f c/s	ΔG -	x -	k cm^{-1}	L cm	$P_R(x)$ -	$P_L(-x)$ -
0		-	-	-	0.4088	0.4088
	0.02041					
1		0.4369	0.1308	7.645	0.4562	0.3051
	0.100					
2		0.4968	0.2305	4.338	0.4540	0.2901
	0.294					
5		0.6219	0.4801	2.083	0.4407	0.2597
	0.0237					
10		0.6983	0.8327	1.201	0.4267	0.2418
	0.0452					
20		0.8136	1.448	0.6904	0.3971	0.2160
	0.0820					
50		0.9734	3.011	0.3321	0.3412	0.1833
	0.0866					
100		1.116	5.239	0.1909	0.2810	0.1572
	0.1710					
200		1.345	9.022	0.1108	0.1778	0.1213
	0.2430					
500		1.642	18.37	0.0544	0.0699	0.0851
	0.0926					
1000		1.812	31.84	0.0314	0.0330	0.0691
	0.0878					
2000		2.006	56.23	0.0178	0.0108	0.0541
	0.1140					
5000		2.305	121.0	0.008	0.0010	0.0369

Figure 6 represents the kinetic energy spectrum of TEST CASE §2 in the wave number domain. The rectangular area below any dotted line is energy in one dimension for the corresponding wave number range. Hand-drawn full line shows the general trend of the spectrum. The insert indicates the (-5/3) slope of the inertial sub-range in the high wave number region.

The numerical results of TEST CASE §8 are in **TABLE 4** with the corresponding spectrum in **Figure 8.** The information used in calculations is generated from a figure showing the energy spectrum in the frequency domain for a turbulent flow behind a grid of bars [Hinze J. O., 1959, pp: 61, Figure 1.18]. It is reported that the study and the Figure are the work of Favre [Favre A. et al., Recherche Aéronaut.., 32; p: 21, 1953].

The measurements are conducted behind a 2.5 cm mesh-size grid, made with cylindrical bars of 0.5 cm diameter. The measurement point was at 40 mesh-size from the grid where turbulence was probably isotropic. Complementary information about the flow is supplied at the heading of **TABLE 4.**

The study of columns reveals that trends observed for TEST Case §2 prevail also for grid turbulence. The wave length corresponding to 1.00 c/s is 0.6 cm which is comparable with grid-bar-diameter (this may be accidental) and is almost ¼ of the mesh size. Fluctuating velocities have amplified almost by a factor of ten, whereas trends of PDF values are similar to those of TEST Case §2.

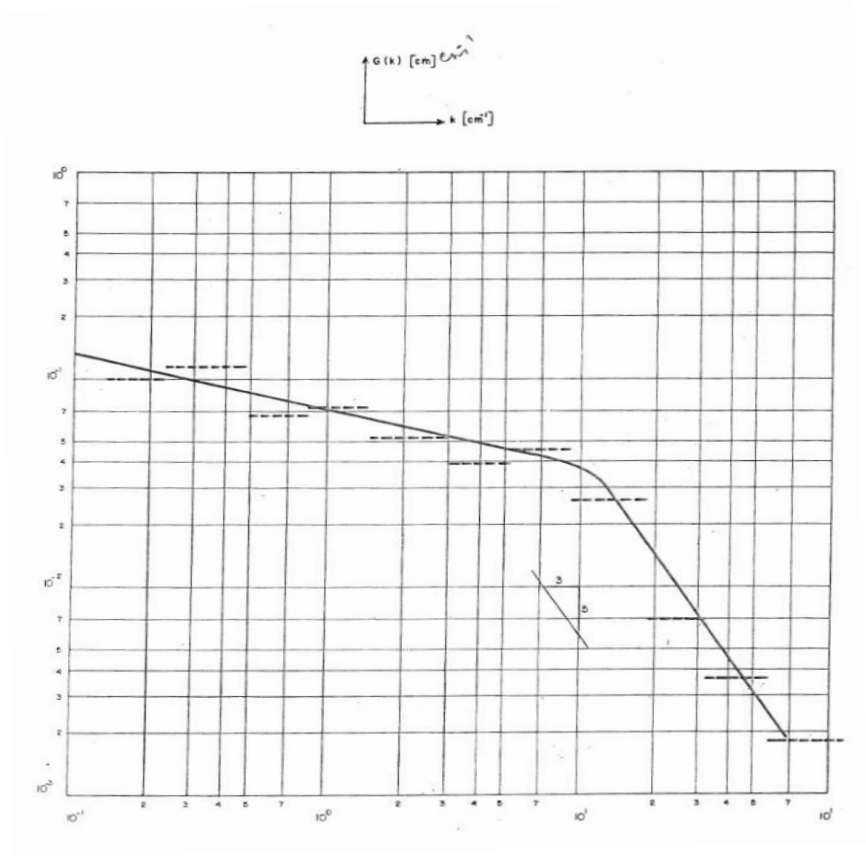

Figure 6: One-dimensional spectrum of TEST Case §2 in wave number.

The measurement system was composed of 55DO1 DISA constant temperature hot-wire anemometer, high and low pass filters of a DISA 55D25 Auxiliary unit, 55D35 rms meter and HP 322 Dual Channel recorder [Çıray C., 1980].

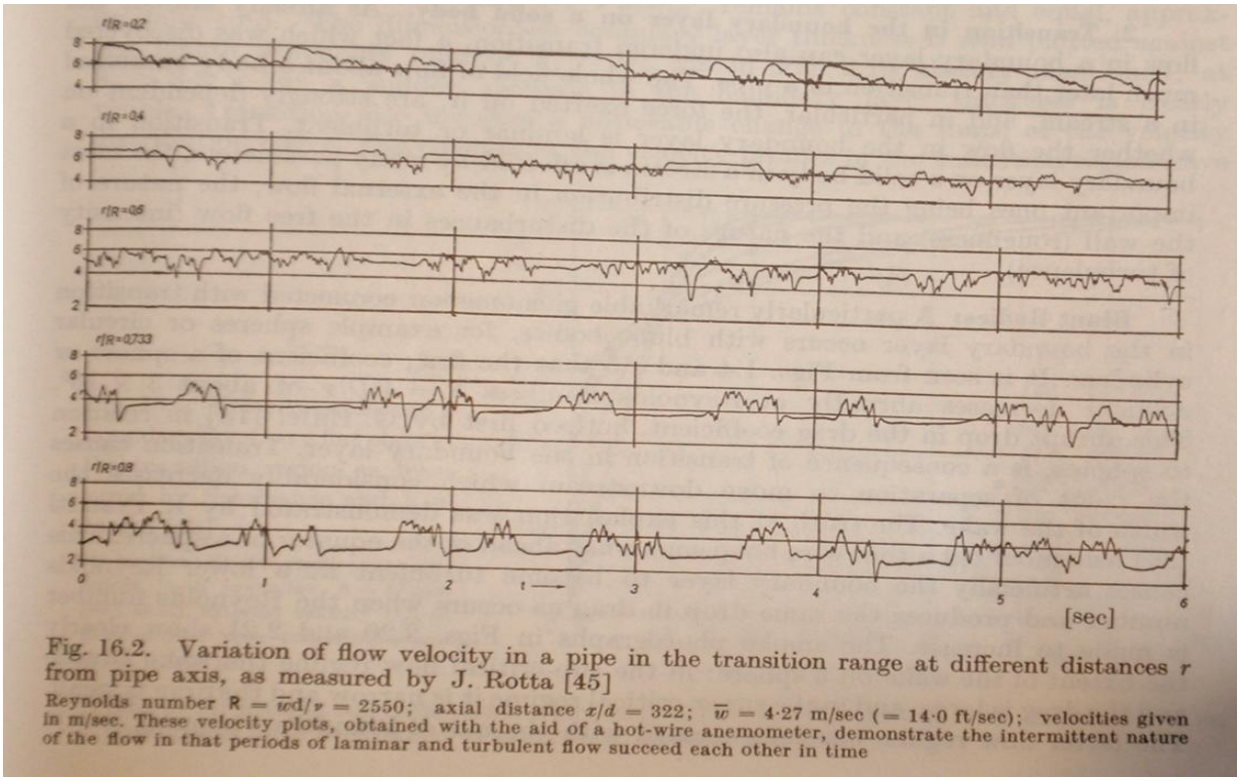

Fig. 16.2. Variation of flow velocity in a pipe in the transition range at different distances r from pipe axis, as measured by J. Rotta [45]

Reynolds number $R = \overline{w}d/\nu = 2550$; axial distance $x/d = 322$; $\overline{w} = 4{\cdot}27$ m/sec (= 14·0 ft/sec); velocities given in m/sec. These velocity plots, obtained with the aid of a hot-wire anemometer, demonstrate the intermittent nature of the flow in that periods of laminar and turbulent flow succeed each other in time

Figure 7: [Schlichting H., 1960].

(This is a very low Reynolds number air flow (R_E =2550) in a pipe of approximately 0.6 cm in diameter.)

TABLE 4: Data and Characteristics of TEST CASE §8

$\overline{U}$ = 12.25 m/s I_{actual} = 0.0200 n = 63 A = 0. 991485

u' = 24.5 cm/s $I_{n=63}$ = 0.0199 $P(1)$ = 0.4104

f c/s	ΔG -	x -	k cm^{-1}	L cm	$P_R(x)$ -	$P_L(-x)$ -
0		-	-	-	0.4104	0.4104
	0.00298					
1		0.2270	1.666	0.6002	0.4502	0.3563
	0.00298					
2		0.2841	2.668	0.3748	0.4565	0.3418
	0.00893					
5		0.3854	4.963	0.2015	0.4630	0.3157
	0.0149					
10		0.4862	7.900	0.1266	0.4625	0.2899
	0.0298					
20		0.6157	12.55	0.7970	0.4504	0.2579
	0.0893					
50		0.8469	23.05	0.0434	0.3945	0.2055
	0.130					
100		1.069	36.41	0.0275	0.3053	0.1623
	0.186					
200		1.317	57.87	0.0173	0.1879	0.1227
	0.290					
500		1.656	109.88	0.0091	0.0608	0.0822
	0.134					
1000		1.893	181.70	0.0055	0.0177	0.0614
	0.0595					
2000		2.058	311.30	0.0032	0.0057	0.0500
	0.0513					
5000		2.231	669.40	0.0015	0.0012	0.0401

Dispersion Relation

Dispersion relation, the relation between the frequency "f" and the wave number "k" can be obtained from numerical results displayed in **TABLES** of Test Cases. These relations are shown in graphical form for eight of ten TEST CASES in **Figure 9**. The frequency range is: $1 < f < 10^4$ c/s. The straight-line relationship between "f" and "k" in log-log coordinates seen in **Figure 9**, suggests the dispersion relation to be of the form:

(10) $$f = Ck^{\beta}.$$

Two constants "C" and "β" can be determined either from **TABLES** of Test Cases or from **Figure 9**. The power "β" is the "dispersion coefficient" reported in **TABLE 5** for two ranges of "f" for which the log-log linearity appears to be a good fit.

Fluctuating Velocity is Inversely Proportional to Wavelength.

With the help of (1), from (10) we can obtain:

(11) $$u = \beta Ck^{\beta-1} = \beta \frac{f}{k}.$$

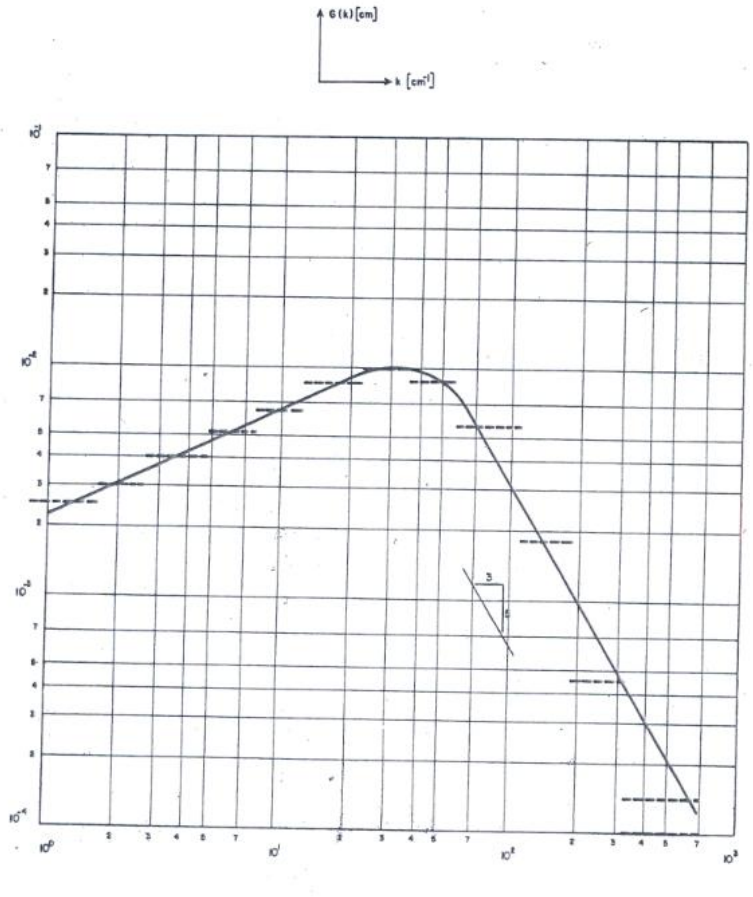

Figure 8: One-dimensional spectrum of TEST CASE §8 in wave number.

The information for TEST CASE §8 is for a turbulent flow behind a grid made of 5 mm cylindrical bars with a mesh size of 2.5 cm. The data belongs to a paper by Favre, [Hinze J. O., 1959, pp: 61, Figure 1.18].

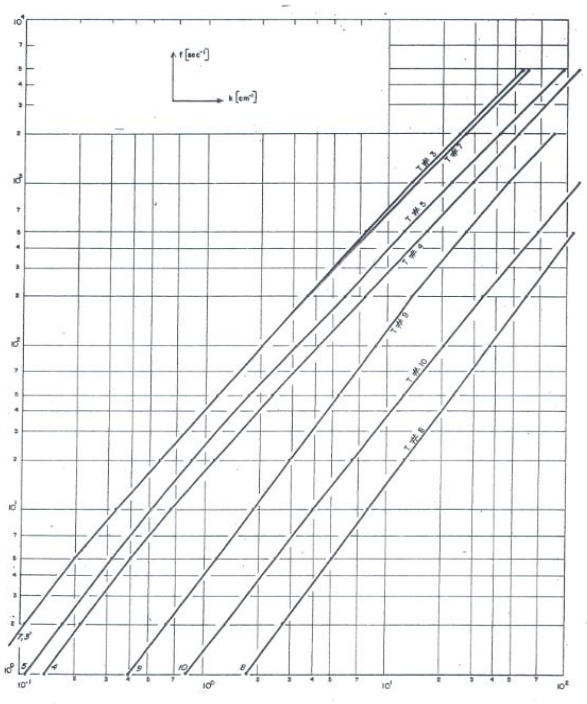

Figure 9: **Dispersion relations for eight of studied ten TEST CASES.**

(Cases §1 and §6 are omitted for a clearer figure.)

TABLE 5: Dispersion Coefficient (β)[3]

TEST §	Lower Range	Higher Range
-	1-100 (or 1- 500) c/s	500-5000 c/s
1	1.8450	1.2240
2	1.2438	1.2210
3	1.4125	1.1625
4	1.4641	1.1682
5	1.4837	1.1520
6	1.8215	1.1325
7	1.5221	1.1325
8	1.4793	1.2723
9	1.5083	1.2107
10	1.4577	1.1628

It seems necessary to point out the difference between "*u*" and "*f/k*". Whereas the former is the group velocity of the group of waves centered around the wave number "*k*" and frequency "*f*", the latter is the phase velocity of the single wave with wave number "*k*" and the frequency "*f*". In conjunction with (11), one can write:

$$u \propto k^{\beta-1}$$

We define "α": $\alpha = \frac{1}{\beta - 1}$. Then:

(12) $$u^{\alpha} \propto \frac{1}{L}$$

where "*L*" is the wave length. The values of "α" ranges are as follows:

$1.0 < \alpha < 4.0$ for $1 < f < 100$ (or 500) c/s and

$3.7 < \alpha < 7.5$ for $500 < f < 5$ kc/s.

It is concluded that the magnitude of fluctuating velocity is an inverse function of eddy size.

The Rate of Decay of Kinetic Energy of Turbulence

The rate of decay of kinetic energy of turbulence is reported to be:

(13) $$\frac{du^2}{dt} = -\frac{Au^3}{L}$$

on grounds of experimental evidences obtained from turbulent flow generated behind a grid [Batchelor, 1960, p: 103].

"A" is a number of the order of unity which may vary slightly with the time of decay and the initial conditions of the turbulence and the choice of L" quotes Batchelor, [Batchelor, 1960, p: 103].

The relation (13) is used to express "*A*" which is a pure number:

(14) $$-\frac{\frac{du^2}{dt}}{\frac{u^3}{L}} = A$$

Figure 10 shows "*A*" for different mesh Reynolds numbers at different distances from the grid as reported in the reference cited.

In view of the QBT approach, one can express the energy transport with a decreasing trend as;

[3] Values of "β" in this Table are inverses of corresponding values in [Çıray C., 1980].

(15) $$\frac{\partial u_G^2}{\partial t} = -u_G \frac{\partial u_G^2}{\partial t} + \dots$$

The fluctuating velocity (group velocity) is symbolized with "u_G" to distinguish it from "u" in Batchelor formulation. The relation (15) is converted to:

(16) $$\frac{\partial u_G^2}{\partial t} \propto -u_G \frac{u_G^2}{L}$$

"u_G" is transformed using (11): $u_G = \beta \frac{f}{k} = \beta u$, where "u" is the phase velocity. We reach:

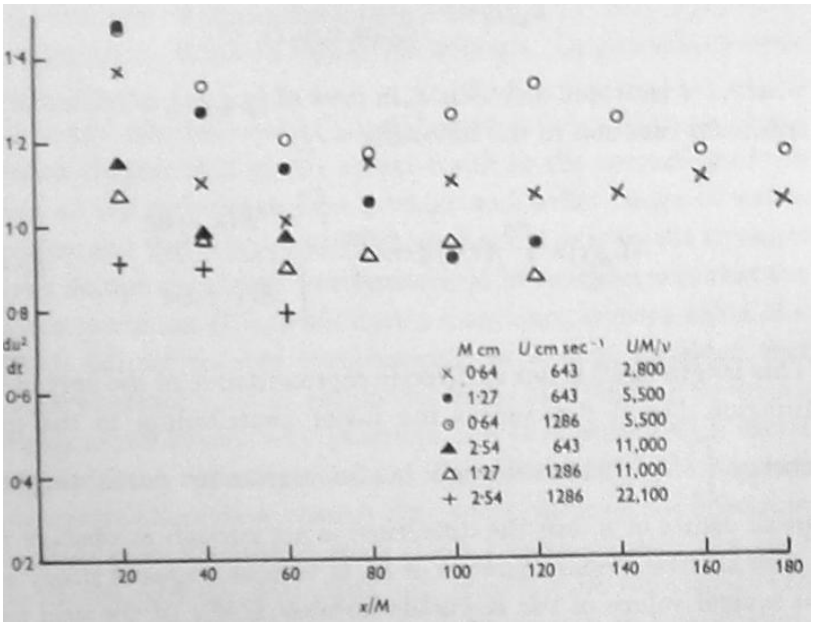

Figure 10: **[Batchelor, 1960, p: 106][4].**

(17) $$\frac{1}{u_G^2}\frac{\partial u_G^2}{\partial t} = -\frac{1}{u^2}\frac{\partial u^2}{\partial t} \propto \beta \frac{u}{L}.$$

Therefore, the relation (17) becomes:

(18) $$\frac{\partial u^2}{\partial t} \propto -\beta \frac{u^3}{L} \quad \text{or} \quad -\frac{\frac{1}{u^2}\frac{\partial u^2}{\partial t}}{\frac{u}{L}} \propto \beta .$$

The first expression of (18) is similar to (13) and the second to (14). One may conclude that "A" and "β" are quite alike, if not the same. The range of "A" (estimated from **Figure 10**) and "β" calculated from dispersion relation are given below:

$$0.80 \le A \le 1.50,$$

$$1.13 \le \beta \le 1.85.$$

Data in **Figure 10** are obtained from the decaying period of turbulent flow behind a grid. Data related to "β" belong to the whole range of spectra and for a variety of flows including grid turbulence, pipe flows, and boundary layers. It is remarkable that "β" of TEST CASE §8 (*grid turbulence*) is within the range of "A".

[4] It is taken from [Batchelor, 1960]. The data is the work of Dryden [Dryden, 1943].

1: It can be asserted that the manner of transporting the kinetic energy of turbulence, as formulated in (13), is not restricted to the decay period, but at least to all wave numbers and flow types that are considered in this study.
2: The relative kinetic energy is the same whether calculated with "group velocity" or "phase velocity", (17).

The lifespan of an eddy

Since the existence of an eddy begins with the formation of a group of waves and ends with the dispersion of the group, the lifespan of the eddy is as long as the existence of a group of waves. The lifespan "*T*" of the eddy can be estimated by dividing the wavelength by its group velocity, i.e.:

(19) $$T = L / u \ .$$

Two test cases referred to above yield the following values:

	1 c/s	**5000 c/s**
Test Case §2	0.13 s	26 μs
Test Case §8	0.11 s	27 μs

Second Group Results

Whereas the first group is directed to study various types of flows from the QBT approach, the second and third groups study specific flows with the same approach.

The second group results are concerned with a zero-pressure-gradient turbulent B/L developing on a smooth surface in a wind tunnel, under three different Test conditions. Test conditions are labeled "0", "1", and "2".

TEST CASE 0: This test deals with a natural TB/L on the flat plate (canonical Turbulent B/L).

TEST CASE 1: A system of "cutout wings" is mounted upstream of LE to influence turbulence, **Figure 11.**

Figure 11: Cutout Wings, TEST CASE 1 (left) and Solid Wings, TEST CASE 2 (Right)[5].

TEST CASE 2: In this case, the entrance is furnished with "solid wings" with controllable openings. This system induces higher turbulence intensity. Detailed information about the set-up and measurement conditions can be found in E. Doğan [Doğan E., 2016].

Hot-wire measurements are conducted at a station 43M (≅ 348 cm) from the LE of the plate. Though hot-wire measurements are performed at 22 points at this station in the original work, only four of them are considered in the study reported here. These points are named A, B, C, and D. Wall distances of these points vary with TEST CASES. Therefore, their positions are labeled with an indicator of the TEST CASE such as 0A, 3B, and 2D. See **Figure 5** and **TABLE 2** for TEST CASE 0 and **TABLE 5** and **6** respectively for TEST CASES 1 and 2. Points A, points B, and points C are not far from each other in all TEST CASES, but point D positions are highly different. OD point wall-distance is 10.9 cm, for 1D it is 17.2 cm and for 2D is 24.5 cm.

Digitized analog hot-wire measurements at a rate of 20 kc/s were supplied by E. Doğan [Reference cited] and they are treated as "instantaneous velocities" throughout the second and third group presentations of this manuscript. Input quantities for the applications of the QBT approach are generated from these instantaneous velocities.

Flow characteristics at measurement points of TEST CASES cover a wide range. Indeed, the mean velocity varies from a minimum of 2.83 m/s (Point 1A) to a maximum of 10.10 m/s (Point 0D). Turbulence intensity changes in the range of 0.70% (point 0D) to 28.70% (point 2A).

[5] From [Bekoğlu E., 2021]. Original Figure belongs to E. Doğan [Doğan E., 2016].

TABLE 6: Flow Characteristics at measurement points for TEST CASE 1.

Point	y [cm]	U_m [m/s]	u' [cm/s]	I_{act} [%]	I_{calc} [%]	n [-]
Point 1A	0.10	2.83	77.7	27.4	27.4	3.50
Point 1B	0.47	4.29	61.8	14.4	14.4	7.60
Point 1C	3.98	5.71	52.9	9.26	9.26	12.5
Point 1D	17.2	6.13	45.0	7.35	7.35	16.1

TABLE 7: Flow Characteristics at measurement points for TEST CASE 2.

Point	y [cm]	U_m [m/s]	u' [cm/s]	I_{act} [%]	I_{calc} [%]	n [-]
Point 2A	0.08	3.83	110	28.7	28.7	3.31
Point 2B	0.36	5.54	98.0	17.7	17.7	5.97
Point 2C	3.83	7.35	101	13.8	13.8	7.98
Point 2D	24.5	7.98	94.7	11.9	11.9	9.47

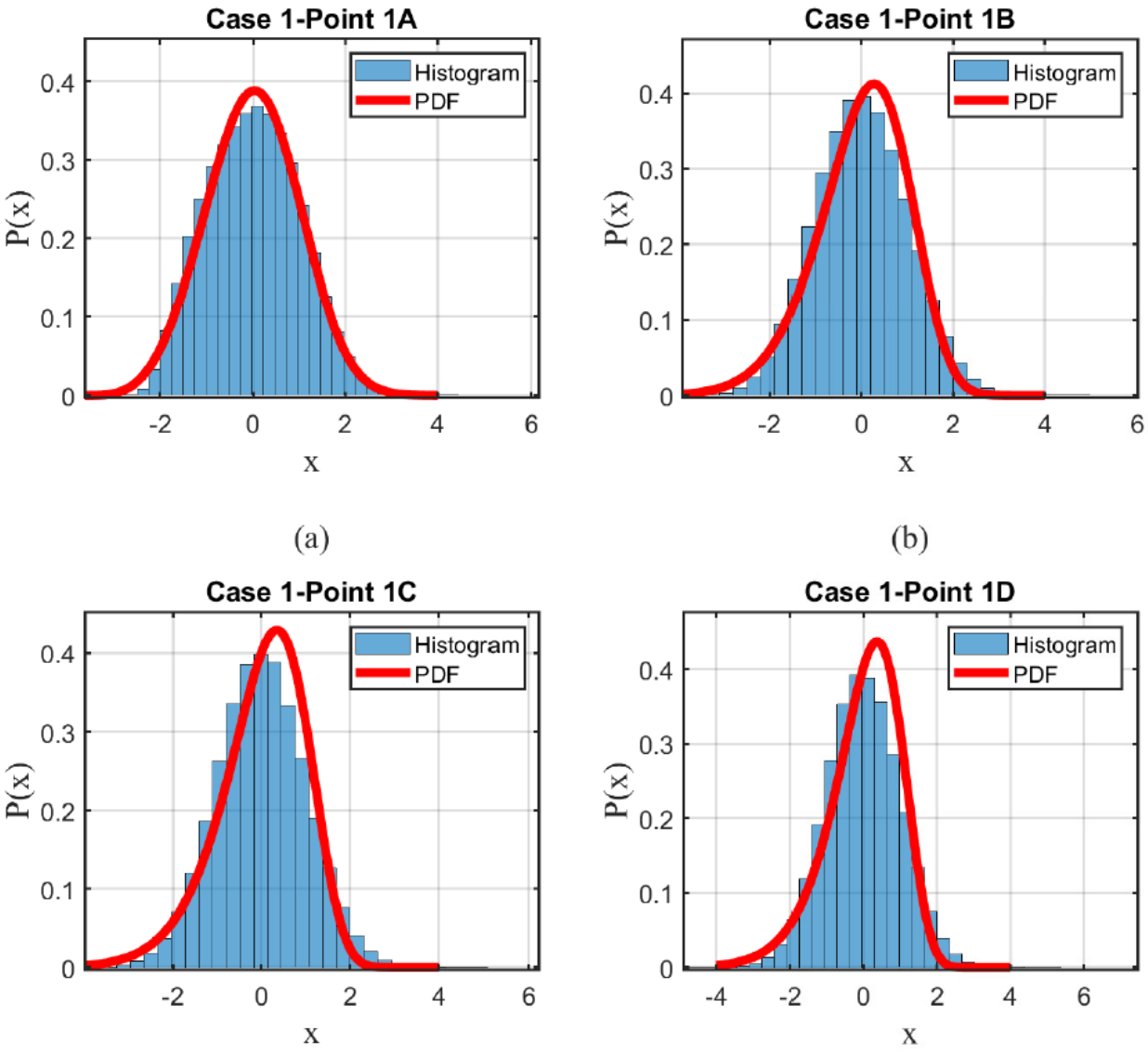

Figure 12: PDF and histograms for TEST CASE 1.

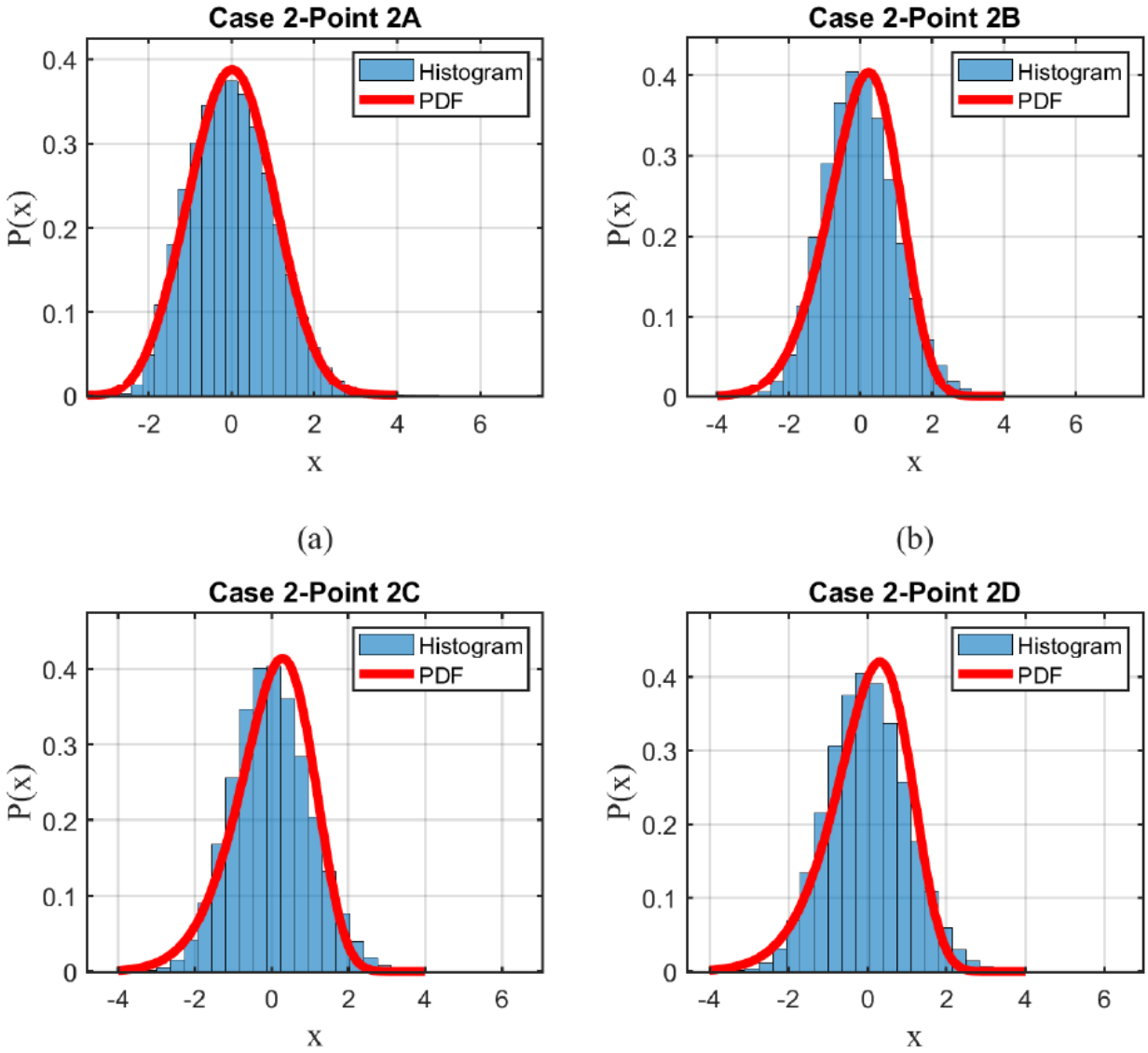

Figure 13: PDF and histograms for TEST CASE 2.

PDF, Relation (7)

In spite of the wide range of variations of flow characteristics described above, the PDF given in equation (7) is satisfactory to represent probabilistic characteristics of fluctuating velocity (hence, instantaneous velocity) as can be observed in **Figures 5, 12,** and **13.**

Eddy-Scale Distributions

Distributions of one-dimensional eddy scales for different frequencies and three TEST CASES are presented in **Figure 14** as a function of wall-distance. **Figure 15** contains the same information but, in terms of non-dimensional wall-distance "y^+".

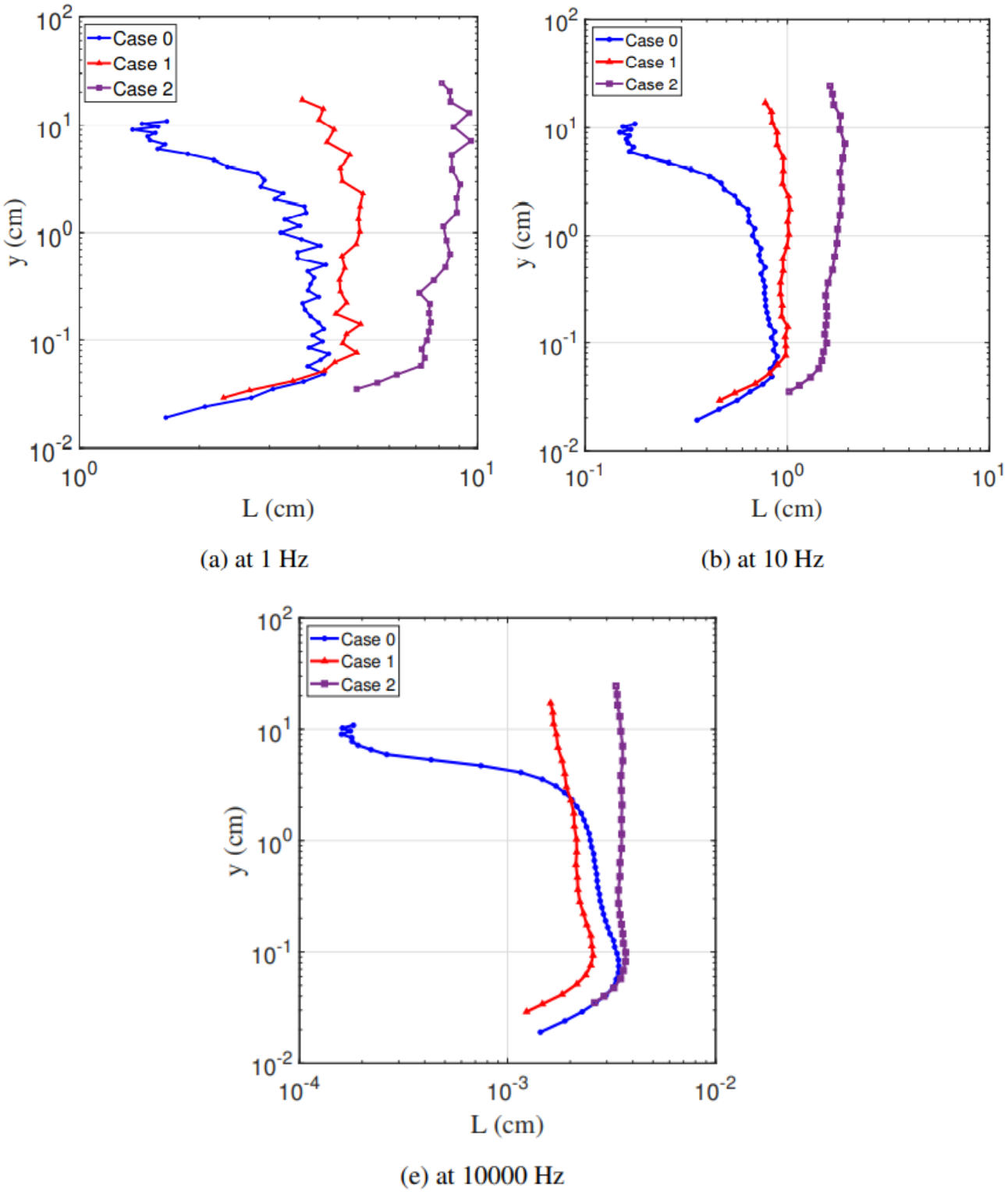

Figure 14: Distribution in "*y*" direction of Eddy-Scales at different frequencies.

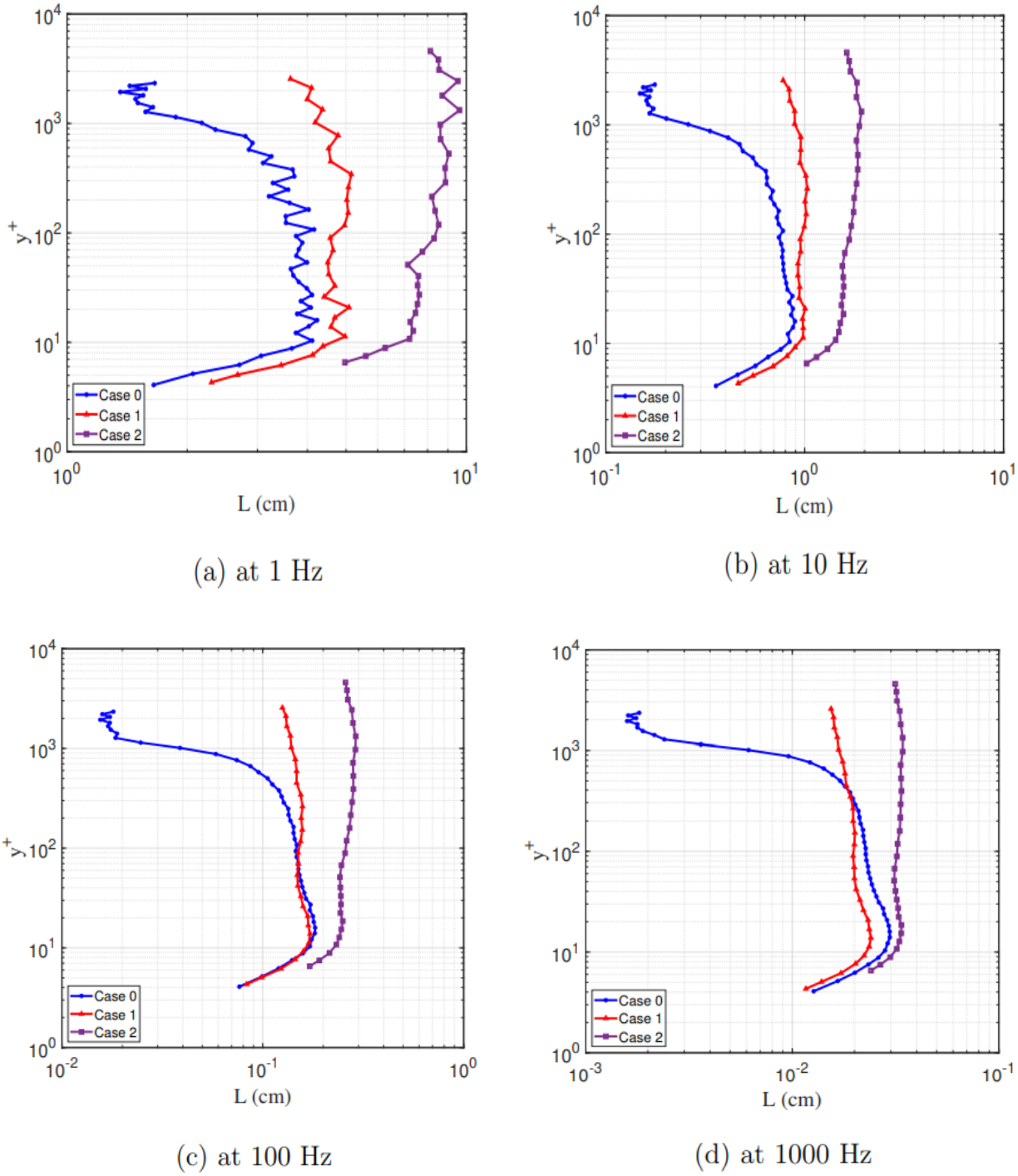

Figure 15A: Eddy-scales along "y^+" at various frequencies and for all TEST CASES.

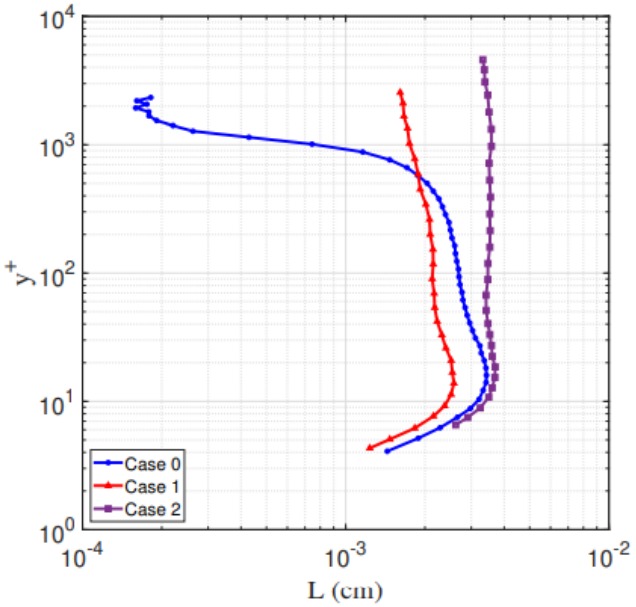

(e) at 10000 Hz

Figure 15B: Eddy-scales along "y^+" for frequency 10000 Hz and for all TEST CASES.

It appears that for all frequencies and for all TEST CASES, at point $y^+ \cong 10$ the slope of the $y^+(L)$ function increases sharply. Until $y^+ \cong 10$ (lower layer) this function increases monotonically in log-log representation. Though viscosity dominates the lower layer, eddies of 1.2 cm at (0A) $y^+ = 4.0$, of 2.2 cm at (1A) $y^+ = 4.5$, and of 5.0 cm at (2A) $y^+ = 6.0$ are observed for 1.0 c/s[6].

The general trend of $y^+(L)$ above $y^+ = 10.0$ (upper layer) reflects an almost constant eddy size for all cases and frequencies, yet specific to TEST CASE and frequency. The constancy indicates that freestream turbulence (FST) introduced at the entrance and all along the depth of the flow has reached a certain dynamic equilibrium. Which station this equilibrium has begun, remains to be explored.

Eddies generated in TEST CASE 1 (cut-out wings) are larger than those of TEST CASE 0, for small frequencies (no FST), **Figures 15a and b**. But differences diminish with increasing frequency and become smaller for frequencies 100 c/s and larger ones, **Figure 15c, d, and e.** One infers that cascading in TEST CASE 1 is more vigorous than NO-FST TEST CASE. Perforations of different diameter holes of cut-out wings create eddies of different scales at the on-set and they may be the cause of an earlier or more effective cascading.

Energy Spectra in Wave Number

Energy spectra in wave number at points A, B, C, and D are illustrated in **Figures 16a, b, c, and d.** Any of these illustrations contains spectra at these points for all three TEST CASES in order to exhibit differences or similarities.

Different energy levels before peak points of $G(k)$, i.e.; in the Large Eddies region, appear as they should be. On the other hand, coalescence towards high wave numbers (Universal Equilibrium region) of the same function is typical for TEST CASES 1 and 2, **Figure 16**. It can be concluded that FST enhances cascading when compared to no-FST case. Inertial-subrange can also be observed for all cases though their extent is small.

The separation of $G(k)$ towards higher wave numbers of TEST CASE 0 from FST cases is noticeable. It is observed that cascading and dissipation in TEST CASE 1 (cutout wings) is more active in all TEST CASES at points A, B, and C as reported earlier.

[6] This fact reminds once more why the original attribution "Laminar Sublayer" was replaced by "Viscous Sublayer".

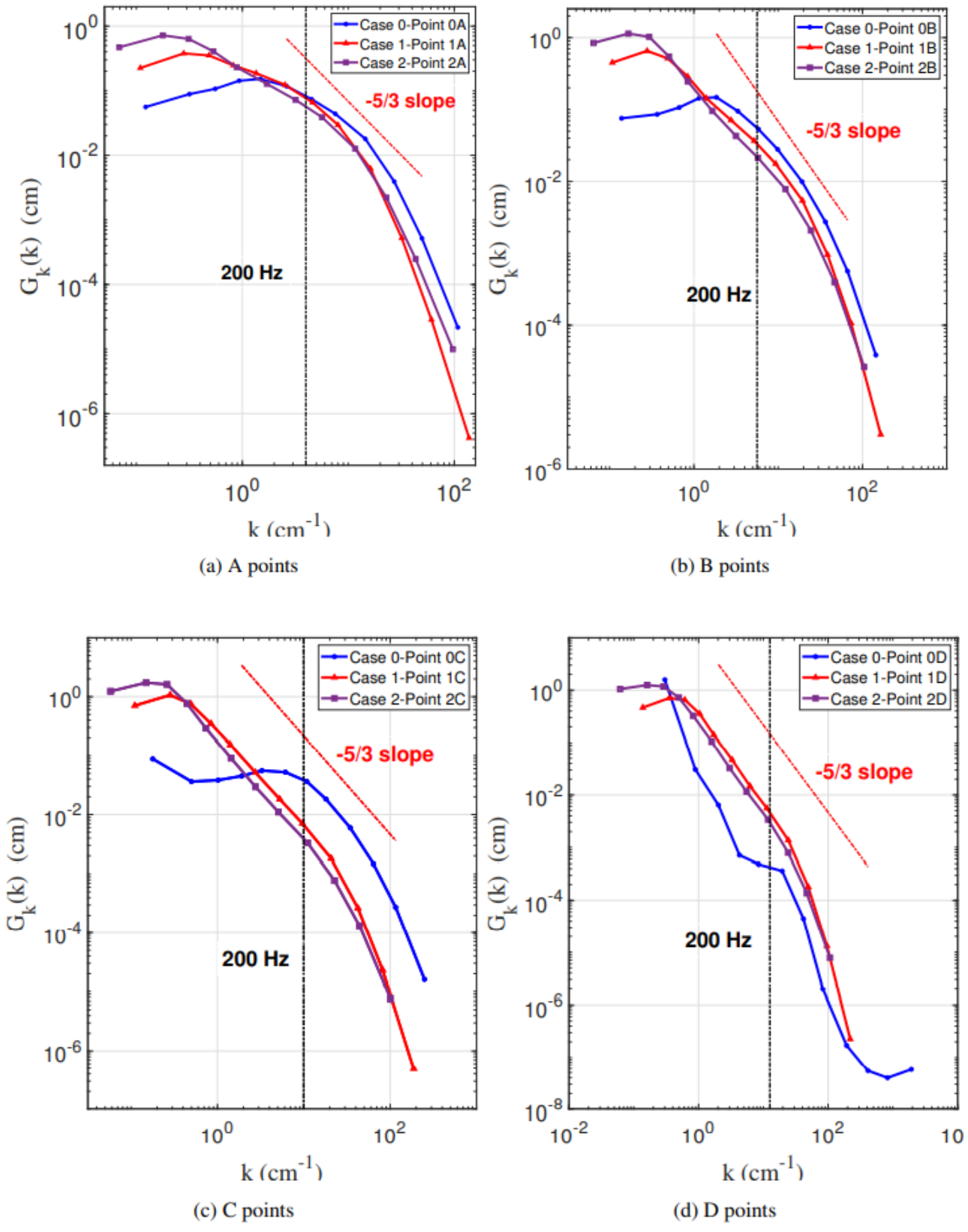

Figure 16: One-Dimensional Energy Spectra for all TEST CASES at four Measurement Points considered in this study.

At point D, the spectrum function for TEST CASE 0 is peculiar in the sense that it does not have the typical *G(k)* of a boundary layer. This is normal since point 0D does not belong to B/L. It is 10.9 cm from the plate whereas the B/L is 5.5 cm thick. It has a "palier" around the wave number 10 cm^{-1} separating the flow into two zones. The upper zone is highly influenced from external flow and energy concentration is high almost reaching the concentration levels of TEST CASES 1 and 2.

The lower zone has the normal appearance of a *G(k)* of a boundary layer flow. Yet, while *G(k)* decreases regularly with high wave numbers, it shows an increasing trend after k = 10^3 cm^{-1}. This may be due to energy transported by entrained eddies from ambient flow.

On the other hand, *G(k)* of TEST CASES 1 and 2 are typical energy spectra of boundary layer flows.

Third Group Results

Third Group Results belong to experiments and ensuing calculations for a round jet. It is a non-swirling jet in an unconfined environment. Details of the set-up and hot-wire measurements are described by I. Çolak [Çolak I., 2022]. The results of data reported in the sequel are related to measurements of velocity components along the jet axis and in a region limited to a maximum distance of 2.0D from the nozzle (D = 2.8 cm is the nozzle diameter). **Figure 17** shows the relative mean-turbulent velocity U/U_m. It is observed that even at 2D distance from the nozzle turbulent jet flow is not yet established. Therefore, the measurements reported here belong to the jet **flow-formation-region** just above the nozzle. Velocity vector at measurement points close to the nozzle surface may be three-dimensional requiring 3D measurements by Hot-Wire Anemometry.

Results shown in the sequel are submitted for the sake of completeness of the work.

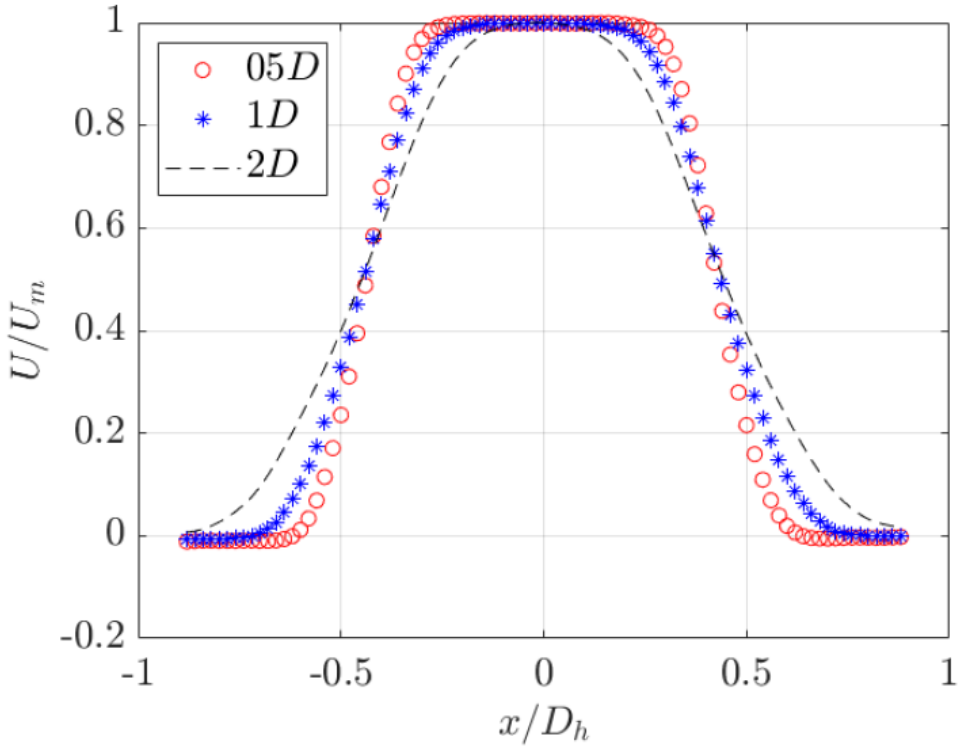

Figure 17: Mean Turbulent Velocity Measurements of a Non-Swirling Round Jet in an Unconfined Environment (Radius of the nozzle: D_h = 1.4 cm).

PDF, Relation (7)

Red full lines representing the PDF (7) are closer to confirm histograms for measurements far from the vicinity of the nozzle. Indeed, at a distance of 0.3D from the nozzle there is concordance only at 10D and 14D from the axis of the jet, **Figures 18c** and **18d**. Similar behavior is observed at 1D from the nozzle surface for radial distances 10D and 14D, **Figures 19Bc and 19Bd.**

In general, accentuated discordance appears in the vicinity of $\pm x = 0$, corresponding to large scale structures at measurement points performed along the axis, **Figures 18a,18b, 19Aa, and 19Ab.**This may be attributed to the fact that the jet-flow-formation region is appreciably three-dimensional.

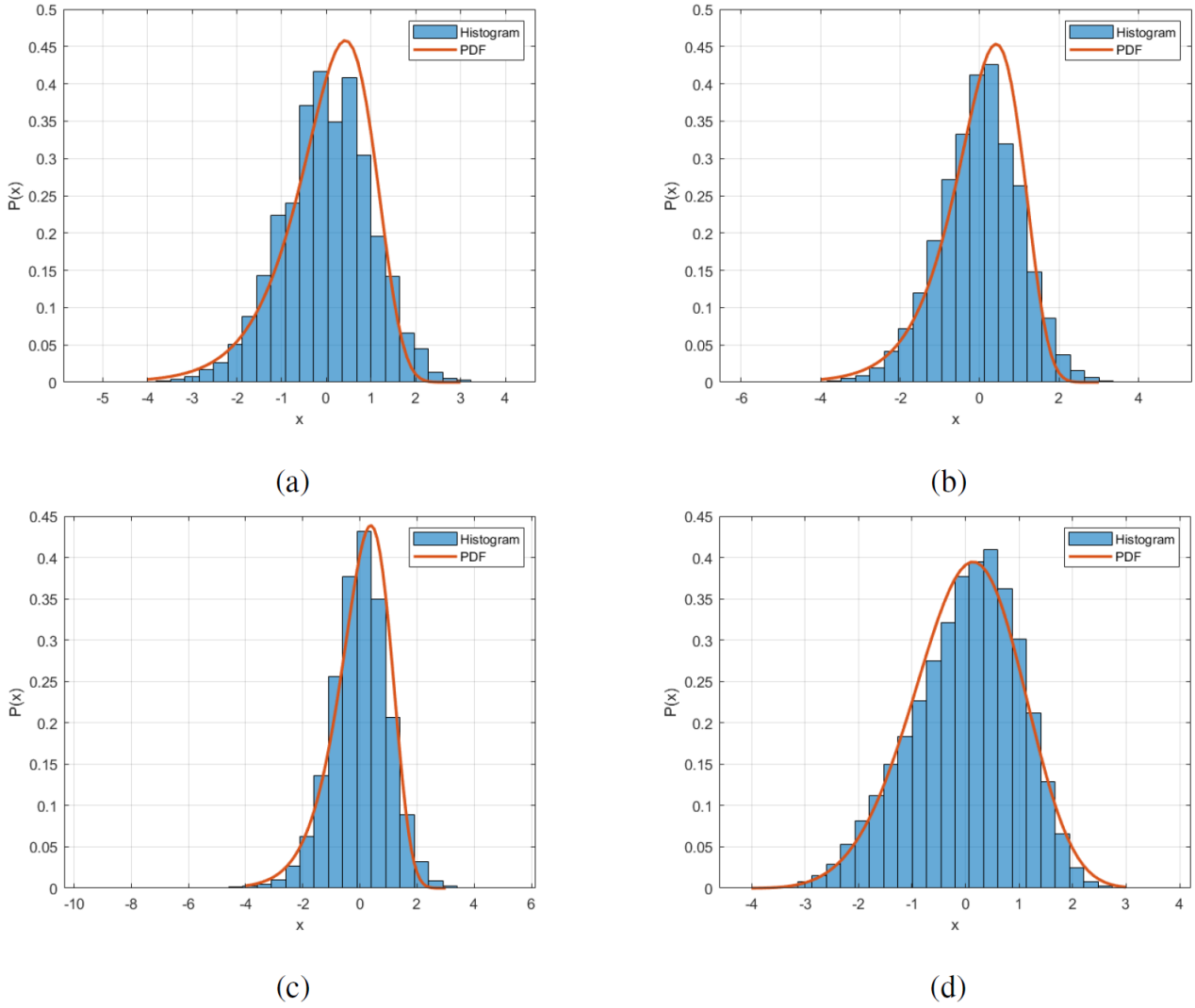

Figure 18: Histograms and PDF's at a distance 0.3D from the nozzle plane and at positions: (a) 0.0 mm; (b) 6.0 mm; (c) 10.0 mm; (d) 14.0 mm from the axis.

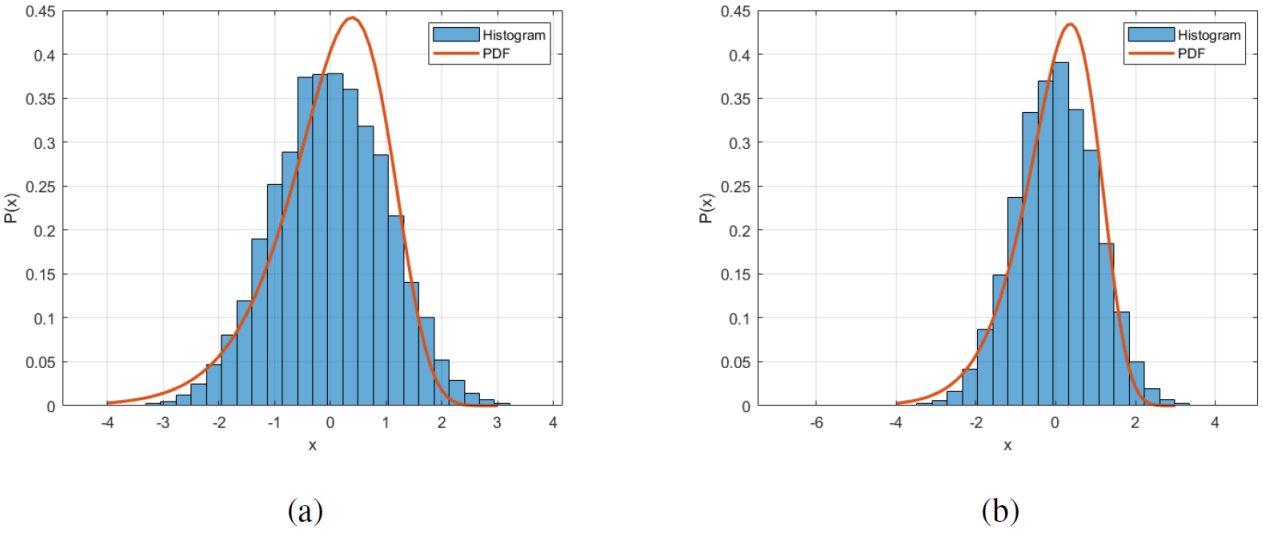

Figure 19A: Histograms and PDF's at a distance 1.0D from the nozzle plane and at positions: (a) 0.0 mm; (b) 6.0 mm.

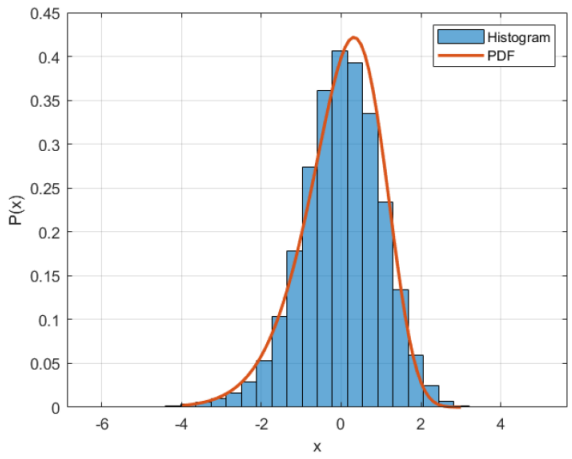

(c)

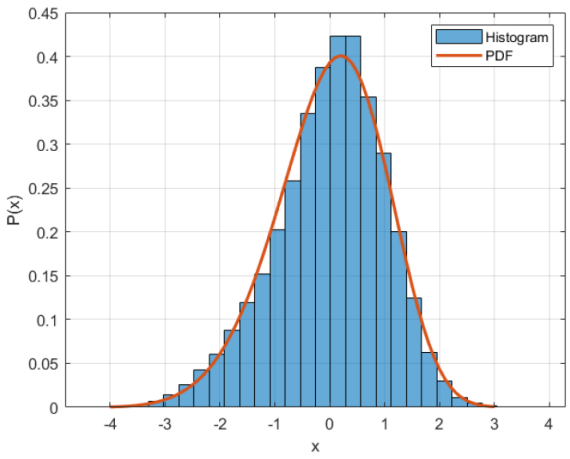

(d)

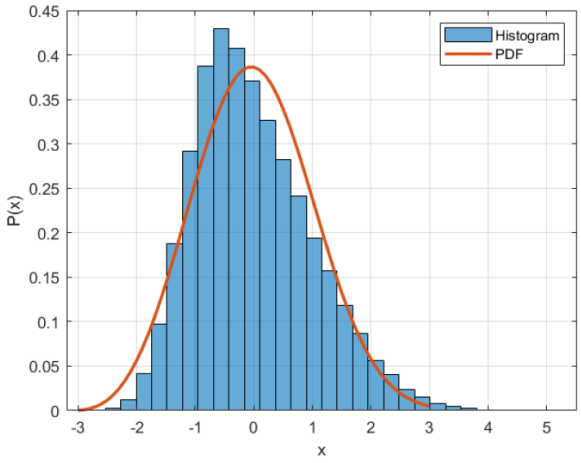

(e)

Figure 19B: Histogram and PDF at a distance 1.0D from the nozzle plane and at positions: (c) 10.0 mm; (d) 14.0 mm and (e) 18.0 mm from axis.

Energy Spectra in Terms of Wave Number

Spectra calculated at various positions in planes 0.3D, 0.5D, and 1.0D distances from the nozzle plane are shown in **Figure 20.**

Energy spectra are peaky in the vicinity of the jet axis and reach the highest energy concentrations, *G(k)*, at the jet axis.

Reynolds numbers based on the distance from the nozzle plane are respectively 8.4×10^3, 14.0×10^3, and 28.0×10^3 for plane distances 03D, 0.5D, and 1.0.D from the nozzle plane. At these Reynolds numbers, the formation of a "universal equilibrium region" is not expected as observed in graphs of Figure 20.

The increasing energy level at both ends of the spectra is peculiar. These are attributed to the three-dimensionality of flow region as suggested in explaining PDF discordance in the previous section and observed in the spectrum at point 0D of non-FST boundary Layer case as seen in **Figure 16d**.

Spectral analysis shows that eddies scale between approximately 5.00 cm which is commensurate with nozzle diameter (= 2.8 cm) and 20.0 μm.

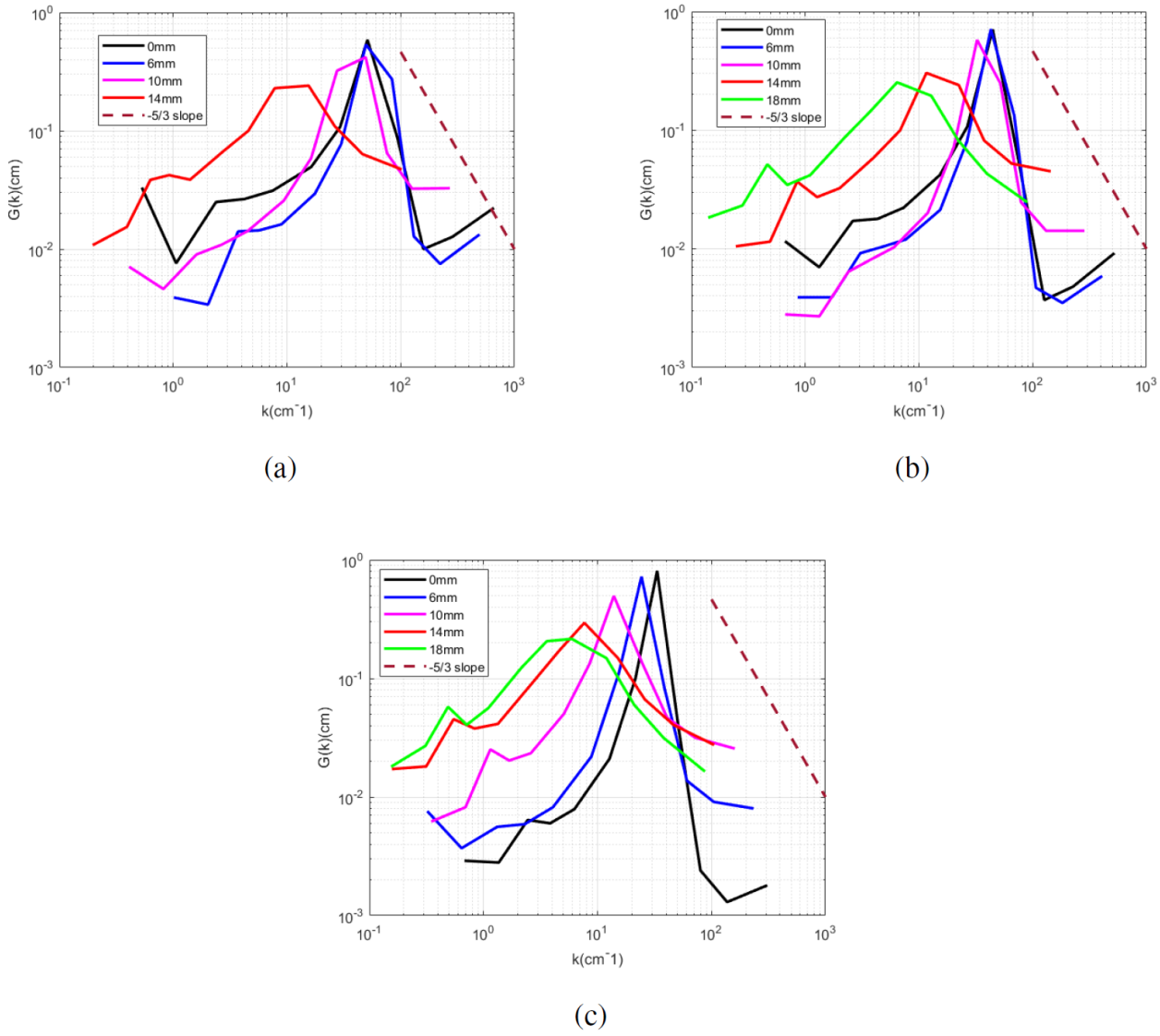

Figure 20: Energy spectra for various measurements in planes at distances a) 0.3D; b) 0.5D and c) 1.0D from the nozzle plane

IN BRIEF

The paradigm of turbulence leading to the Quantic Behavior of Turbulence is a realistic description of the physics of turbulence. Indeed, three basic items of this approach tested in various flows and explained above, support this view.

1: Particle characteristics such as the streamwise wave numbers of eddies satisfy intrinsic conditions of turbulence. The calculation uses a unique method for the whole range of the spectrum.

2: Wave-like behavior of turbulence leading to define fluctuations as group velocity leads to obtain turbulence dispersion relation and lifespan of eddies.

3: The PDF of fluctuations used in the calculation is a modified form of the Maxwell-Boltzman relation to estimate the speed of molecules conforms with histograms of velocity fluctuations. This leads to think that turbulence has its roots in molecular activity.

The application of QBT in three dimensions and to extend the molecular simulations to reach higher Reynolds numbers in micro-tubes will be the following stage of this subject.

Acknowledgement

We appreciate and thank Dr. Eda Doğan for the permission to use her original data of Turbulent Boundary Layer referred as [Dogan E., 2016]. We are equally thankful to Mr. Kıyıcı F. and Mr. Gencer B. for allowing us to use their original data on the Jet Flow analysis referred as [Kıyıcı F. and Gencer B., 2016].

References

[Batchelor G. K., 1960] "The Theory of Homogeneous Turbulence". Cambridge at the University Press, 1960.

[Bekoğlu E., 2021] "A Study to Evaluate Scales in some Turbulent Flows in view of Quantic Behavior of Turbulence using Experimental Results". MS Thesis, Aerospace Engineering Department, METU, 2021.

[Çıray C., 1980] "On Wave Number Definition". METU Journal of Pure and Applied Sciences. Vol.13. No:3. pp: 431-488. December 1980, (this issue of the Journal appeared in 1982).

[Çıray C., 2017] "Wave Number in Turbulence and Its Discrete Nature". 9. Ankara, International Aerospace Conference. AIAC 2017- 0041.

[Çolak I. 2022] "A Study of Turbulence Characteristics of some Turbulent Flows using experimental data with Application of Quantic Behavior of Turbulence". MS Thesis, Aerospace Engineering Department, METU, 2022.

[de Broglie., 1974] Proof by "de Broglie" is given in "Introduction to Molecular Structure and Thermodynamics" of F. P. Incropera. John Wiley and Sons, 1974. p: 40-41.

[de Kat R. and Ganapathisubramani B., 2015] Frequency-wave number mapping in turbulent shear flow. J. of Fluid Mech. (2015), Vol. 783, pp. 166-190. Cambridge University Press, 2015.

[Doğan E., 2016] E. Dogan, R. Hanson and B. Ganapathisubramani. Interaction of large-scale free stream turbulence with turbulent boundary layers. Journal of Fluid Mechanics, pages 1-29, 2016.

[Dryden H. L. D., 1943] A Review of Statistical Theory of Turbulence Quarterly Applied Mathematics I, 7.

[Eneren Ş. P., 2016] Validation of a Particle Simulation Approach. MS. Thesis. Aerospace Eng. Department. METU, 2016.

[Favre A. et al., 1953] Recherche Aéronaut…., 32; p:21, 1953

[Hinze J. O., 1959] Turbulence, an Introduction to its Mechanism and Theory. McGraw Hill. 1959.

[Kabakci I., 2019] Applications of a Simulation Approach,. MS. Thesis. Aerospace Eng. Department. METU. 2019.

[Kai Schneider and Oleg V. Vasilyev, 2010] Wavelet Methods in Computational Fluid Dynamics, Annual Review of Fluid Mechanics, Volume 42 p: 473-503. 2010. Editors: S.H. Davis and P. Moin.

[Kıyıcı F. and Gencer B] "Jet Flow Analysis". Private Communication. Institute of Wind Engineering, METU, 2021.

[Lamb H., 1962] Hydrodynamics, Sixth Edition, Cambridge at the University Press, 1962. Article 236, p: 380-382.

[Landau-Lifshitz, 1959] Fluid Mechanics. Pergamon Press, 1959.

[Lele S. K., 1994] Compressibility Effects on Turbulence. Annual Review of Fluid Mechanics, vol. 26. 1994. pp: 211-254.

[Prandtl L. Z., 1925] Angew. Math. und Mech. 5, 136. 1925.

[Reynolds O., 1883] "An experimental investigation of the circumstances which determine whether the motion of watershall be direct or sinuous, and of the law of resistance in parallel channels". Philosophical Transactions, 174; 1883. s. 935-982.

[Schlichtingh H., 1960] Figure 4 is copied from H. Schlichting's Boundary Layer Theory, fourth edition, McGraw Hill Co. INC, 1960, page 377. It is reported from J. Rotta's paper in Ing. Archives **24**, 258-281 (1956).

[Taylor G. I., 1915] Philosophical Transactions **A**, 215 (1915), 1-26.

[Taylor G. I., 1938] The Spectrum of Turbulence. Proceedings of Royal Society, London **164** (919).

[Whitham G. B., 1974] Linear and Nonlinear Waves. John Wiley and Sons, 1974. p:10 and Chapter 11.

APPENDIX: MATHEMATICS RELATED TO QUANTIC BEHAVIOR OF TURBULENCE

Cahit Çıray

INTRODUCTION. This Appendix contains details of mathematical developments that was not possible to include to QUANTIC BEHAVIOR OF TURBULENCE.

CONTENT

I. GENERAL.

I.1. Definitions.

U : Instantaneous velocity; u : Fluctuating velocity

$\overline{U}$: Mean velocity; $u' = \overline{u^2}^{1/2}$: rms of u

$$U = \overline{U} + u = \overline{U}\left(1 + \frac{u}{\overline{U}}\right) = \overline{U}\left(1 + \frac{u'}{\overline{U}}\frac{u}{u'}\right) = \overline{U}(1 + Ix) = y\overline{U} \ ;$$

$$x = \frac{u}{u'} \ ; \quad y = \frac{U}{\overline{U}} = 1 + Ix \ ; \quad I = \frac{u'}{\overline{U}}$$

$P(y)$: PDF, a function that is known.

$G(f)$: Spectrum function normalized with u'^2. It is numerically available from experiments.

ω : Circular frequency, $\omega = 2\pi f$.

f : Frequency in c/s.

μ^κ : Normalized κ^{th} moment of "U":

$$\mu^\kappa = \frac{1}{\overline{U}^\kappa}\int_{-\infty}^{\infty} P(y)U^\kappa dy \ .$$

I.2. PDF Properties and Consequences.

(1): $\int_{-\infty}^{\infty} P(y)dy = 1 \ \therefore$ (1A): $\int_{-\infty}^{\infty} P(x)dx = \frac{1}{I}$

(2): $\int_{-\infty}^{\infty} P(y)Udy = \overline{U} \ \therefore$ (3): $\int_{-\infty}^{\infty} P(y)ydy = 1$

$$\therefore \int_{-\infty}^{\infty} P(y)Udy = \int_{-\infty}^{\infty} P(y)\left(\overline{U} + u\right)dy = \overline{U}\int_{-\infty}^{\infty} P(y)dy + \int_{-\infty}^{\infty} P(y)udy = \overline{U}$$

$\therefore \ \overline{U} + \int_{-\infty}^{\infty} P(y)udy = \overline{U}$. Hence:

(4): $\int_{-\infty}^{\infty} P(y)udy = 0$ and (5): $\int_{-\infty}^{\infty} P(1 + Ix)udx = 0$.

$\int_{-\infty}^{\infty} P(y)U^2 dy = \int_{-\infty}^{\infty} P(y)\left(\overline{U} + u\right)^2 dy = \overline{U}^2 \int_{-\infty}^{\infty} P(y)dy + \int_{-\infty}^{\infty} P(y)u^2 dy = \overline{U}^2 + u'^2$. Hence: (6) $\mu^2 = 1 + I^2$

II. CONSTANTS OF PDF.

II.1. Expression of PDF.

(7) $$P(y) = P(1)y^n exp\left\{A^n\left(1-y^n\right)\right\}$$

where "*P(1)*" and "*A*" are constants to be found from properties of PDF. "*n*" will be determined for each case. Expansion of (7) yields:

(8) $$P(y) = Cy^n exp\left(-A^n y^n\right)$$

Hence:

(9) $$C = P(1)exp\left(A^n\right)$$

Shortly:

(10) $$P(y) = C\varphi(y)$$

with

(10) $$\varphi(y) = y^n \exp(-A^n y^n)$$

II.2. Finding P(1).

To satisfy the condition (1), we must have:

(12) $$C = \frac{1}{\int_{-\infty}^{\infty} \varphi(y)dy}$$

II.2.1. Integral in (12)

Apply the transformation: $y^n = q$. Then:

(13) $$dy = \frac{1}{n}\frac{q^{\frac{1}{n}}}{q}dq$$

Hence: $\int_{-\infty}^{\infty} \varphi(y)dy = \int_{-\infty}^{\infty} y^n \exp(-A^n y^n)dy = \int_{-\infty}^{\infty} q \exp(-A^n q)\frac{1}{n}\frac{q^{\frac{1}{n}}}{q}dq$

or

(14) $$\int_{-\infty}^{\infty} \varphi(y)dy = \frac{1}{n}\int_{-\infty}^{\infty} q^{\frac{1}{n}} \exp(-A^n q)dq .$$

The RHS of this equation is similar to the equation used for the definition of the $\Gamma(t)$ as given in "Handbook of Mathematical Functions ", edited by M. Abramowitz and I. A. Stegun, Dover publication. The formula appears on page 255 with formula identification: 6.1.1. It reads:

(6.1.1) $$\Gamma(z) = k^z \int_0^{\infty} t^{z-1} \exp(-kt)dt .$$

The lower limits of the two integrals are not the same. But this does not cause a problem since:

$$y \geq 0.$$

Therefore:

$$\int_{-\infty}^{\infty} \varphi(y)dy = \int_0^{\infty} \varphi(y)dy .$$

The correspondence can be established as follows:

(6.1.1)	(14)
t	q
k	A^n

$$z-1=\frac{1}{n} \quad \rightarrow \quad z=\frac{n+1}{n}$$

Then, one can write: $$n\int_{-\infty}^{\infty}\varphi(y)dy=\left(A^n\right)^{-\frac{n+1}{n}}\Gamma\left(\frac{n+1}{n}\right)$$ or:

(15) $$\int_{-\infty}^{\infty}\varphi(y)dy=\frac{1}{n}A^{-(n+1)}\Gamma\left(\frac{n+1}{n}\right)$$

The consequence of (1), i.e.: (12) leads to:

(16) $$C=\frac{nA^{n+1}}{\Gamma\left(\frac{n+1}{n}\right)}$$

and (9) yields:

(17) $$P(1)=\frac{nA^{n+1}}{\Gamma\left(\frac{n+1}{n}\right)\exp\left(A^n\right)}.$$

Hence:

(18) $$P(y)=\frac{nA^{n+1}}{\Gamma\left(\frac{n+1}{n}\right)}y^n\exp\left(-A^n y^n\right).$$

If the same derivation process is used to express *P(y)* in terms of "*x*", the condition (1A) leads to (19) where *y=1+Ix* by definition,

(19)

II.3. Finding "*A*".

The condition (3) is used in conjunction with (8),

(20) $$C\int_{-\infty}^{\infty}\varphi(y)ydy=C\int_{-\infty}^{\infty}y^{n+1}\exp(-A^n y^n)dy=1.$$

The integral on the RHS can be calculated as explained in II.2.1 for (14) .But, in this case:

$$z=\frac{n+2}{n}.$$

The relation (20) becomes:

$$C\frac{1}{n}\Gamma\left(\frac{n+2}{n}\right)\frac{1}{A^{n+2}}=1.$$

Using (16):

$$\frac{nA^{n+1}}{\Gamma\left(\frac{n+1}{n}\right)}\frac{1}{n}\Gamma\left(\frac{n+2}{n}\right)\frac{1}{A^{n+2}}=1.$$

Finally, one arrives to:

$$A = \frac{\Gamma\left(\frac{n+2}{n}\right)}{\Gamma\left(\frac{n+1}{n}\right)}. \tag{21}$$

II.4. Finding "μ^{κ}".

By definition:

$$\mu^{\kappa} = = \frac{1}{\overline{U}^{\kappa}} \int_{-\infty}^{\infty} P(y) U^{\kappa} dy = \int_{-\infty}^{\infty} P(y) y^{\kappa} dy = C \int_{-\infty}^{\infty} y^{n} \exp\left(-A^{n} y^{n}\right) y^{\kappa} dy .$$

We use (8) and obtain:

$$\mu^{\kappa} = C \int_{-\infty}^{\infty} y^{n+\kappa} \exp\left(-A^{n} y^{n}\right) dy \tag{22}$$

The integration of (22) can be performed parallel to II.2, i.e.:

$$y^n = q \quad \text{and} \quad dy = \frac{1}{n} \frac{q^{\frac{1}{n}}}{q} dq .$$

Then:

$$\mu^{\kappa} = \frac{C}{n} \int_{-\infty}^{\infty} q^{\frac{1+\kappa}{n}} \exp\left(-A^{n} q\right) dq . \tag{23}$$

Correspondence with 6.1.1:

6.1.1		(23)
t		q
$z - 1 = \frac{1+\kappa}{n}$	$\rightarrow$	$z = \frac{n+\kappa+1}{n}$
kA^{n}	$\rightarrow$	$k^{-z} = A^{-(n+\kappa+1)}$

Relation (23) becomes:

$$\mu^{\kappa} = \frac{C}{n} A^{-(n+\kappa+1)} \Gamma\left(\frac{n+\kappa+1}{n}\right). \tag{24}$$

Introducing (21) into (24), one arrives to:

$$\mu^{\kappa} = \frac{\left[\Gamma\left(\frac{n+1}{n}\right)\right]^{\kappa-1} \Gamma\left(\frac{n+\kappa+1}{n}\right)}{\left[\Gamma\left(\frac{n+2}{n}\right)\right]^{\kappa}}. \tag{25}$$

III: WORKING EQUATIONS.

III.1. Discrete Form of Working Equations.

The governing equation which is used to obtain *u(f)* is:

$$\int_{-\infty}^{\infty} P(x) u^{2} dx = u'^{2} \int_{0}^{\infty} G(f) df \quad \text{or} \quad \int_{-\infty}^{\infty} P(x) x^{2} dx = \int_{0}^{\infty} G(f) df . \tag{26}$$

It is understood that "+*u*" and "-*u*" may occur at different probabilities but at the same frequency and contribute together to kinetic energy in the band of "*f*".

The PDF used in this study is skew and both, left and right hand have to be considered separately during the integration process of (26). The integration is carried piecewise for a velocity range of $\pm x_i$ to $\pm x_{i\pm1}$ where the associated kinetic energy is ΔG_i in the frequency range f_i to f_{i+1}. Equation (26) becomes:

$$\int_{-x_i}^{-x_{i-1}} P_L(\xi)\xi^2 d\xi + \int_{x_i}^{x_{i+1}} P_R(\xi)\xi^2 d\xi = \int_{f_i}^{f_{i+1}} G(\eta)d\eta. \tag{27}$$

The discrete expression equivalent to (27) is:

$$\left[P_L(-x_{i-1})(x_{i-1})^2 + P_L(-x_i)x_i^2\right]\frac{-x_{i-1}-(-x_i)}{2} + \left[P_R(x_{i+1})(x_{i+1})^2 + P_R(x_i)x_i^2\right]\frac{x_{i+1}-x_i}{2} = \Delta G(f_i; f_{i+1}). \tag{28}$$

We take:

$$x_{i+1} = x_i + \Delta x_{i+1} \quad ; \quad P_R(x_{i+1}) = P_R(x_i) + \frac{dP_R(x_i)}{dx}\Delta x_{i+1} + ...$$

and

$$-x_{i-1} = -x_i - \Delta x_{i+1} \quad ; \quad P_L(-x_{i-1}) = P_L(-x_i) - \frac{dP_L(-x_i)}{dx}\Delta x_{i+1} + ...$$

Then, to first order (28) becomes:

$$\left\{\left[P_L(-x_i) - \frac{dP_L(-x_i)}{dx}\Delta x_{i+1}\right](-x_i - \Delta x_{i+1})^2 + P_L(-x_i)x_i^2\right\}\frac{\Delta x_{i+1}}{2} + \left\{\left[P_R(x_i) + \frac{dP_R(x_i)}{dx}\Delta x_{i+1}\right](x_i + \Delta x_{i+1})^2 + P_R(x_i)x_i^2\right\}\frac{\Delta x_{i+1}}{2} = \Delta G(f_i; f_{i+1}). \tag{29}$$

Keeping terms up to second degree (inclusive) in "Δx_{i+1}", (29) reduces to:

$$C_1 \Delta x_{i+1}^2 + C_2 \Delta x_{i+1} = \Delta G(f_i, f_{i+1}) \tag{30}$$

where:

$$C_1 = x_i\left[P_L(-x_i) + P_R(x_i)\right] + \frac{1}{2}x_i^2\left[-\left.\frac{dP_L}{dx}\right|_{-x_i} + \left.\frac{dP_R}{dx}\right|_{x_i}\right] \tag{30a}$$

$$C_2 = x_i^2\left[P_L(-x_i) + P_R(x_i)\right] \tag{30b}$$

The set of equations (30) form the Working Equations.

III.2. Initiation of Calculation of Working Equations.

III.2.1. Finding "x_1".

The initial value of $x_0 = 0$ and associated PDF value is $P_L(x=0) = P_R(x=0) = P(1)$.

In the vicinity of x_0, to a good approximation:

$$\int_0^{x_1} 2P(1)x^2 dx = \Delta G(0;1).$$

The first non-zero value of "x" is x_1.

Hence: $$2P(1)x_1^2 = \Delta G(0;1).$$

Therefore:

$$x_1 = \left(\frac{3}{2}\frac{\Delta G(0;1)}{P(1)}\right)^{1/3}. \tag{31}$$

Remaining values of "x_i" are found with the help of the set (30) and $x_{i+1} = x_i + \Delta x_{i+1}$.
The result is a relation in numerical form like:

(32) $$x = x(f).$$

II.2.1. Finding "k_1". We remember that:

(33) $$u = \frac{d\omega}{dk}.$$

Using $\omega = 2\pi f$, (33) leads to:

(34) $$k = \int_0^{\omega} \frac{d\omega}{u} = \frac{2\pi}{u'} \int_0^{f} \frac{df}{x}.$$

The following practice is useful if "*x*" is available numerically. Then:

(35) $$k(f) = \frac{2\pi}{u'} \left[\int_0^{1} \frac{df}{x} + \int_1^{f} \frac{df}{x} \right] = k(1) + \frac{2\pi}{u'} \int_1^{f} \frac{df}{x}.$$

In order to find $k(1)$, it is proper to express *x(f)* as:

(36) $$x = x_b \left(\frac{f}{f_b} \right)^B \quad \text{or} \quad x = Mf^B,$$

where "*B*", "x_b" and "f_b" can be determined once the first three (*x* ; *f*) combinations are selected from the list of numerical values of (32). Inserting (36) into the integral expression of *k(1)* in (35), one has:

(37) $$k(1) = \frac{2\pi}{u'} \frac{f_b^B}{x_b} \int_0^{f_1} \frac{df}{f^B}$$

The result is:

(38) $$k(1) = \frac{2\pi}{u'} \left(\frac{f_b}{f_1} \right)^B \frac{f_1}{1-B} = \frac{2\pi}{u'} \frac{1}{M} \frac{f_1^{1-B}}{1-B}.$$

In view of tabulated numerical values of (32), the far end of RHS of (35) is expressed as:

(39) $$k(f_i) = \frac{2\pi}{u'} \left(\frac{f_b}{f_1} \right)^B \frac{f_1}{1-B} + \frac{4\pi}{u'} \sum_{j=2}^{i} \frac{f_j - f_{j-1}}{x_j + x_{j-1}} \quad \text{or}$$

(40) $$k(f_i) = \frac{2\pi}{u'} \left[\left(\frac{f_b}{f_1} \right)^B \frac{f_1}{1-B} + 2 \sum_{j=2}^{i} \frac{f_j - f_{j-1}}{x_j + x_{j-1}} \right].$$